Trends in volumetric-energy efficiency of implantable neurostimulators: a review from a circuits and systems perspective

Santiago Martínez, *Student Member, IEEE,* Francisco Veirano, *Member, IEEE,*
Timothy G. Constandinou, *Senior Member, IEEE,* and Fernando Silveira, *Senior Member, IEEE*

Abstract—This paper presents a comprehensive review of state-of-the-art, commercially available neurostimulators. We analyse key design parameters and performance metrics of 45 implantable medical devices across six neural target categories: deep brain, vagus nerve, spinal cord, phrenic nerve, sacral nerve and hypoglossal nerve. We then benchmark these alongside modern cardiac pacemaker devices that represent a more established market. This work studies trends in device size, electrode number, battery technology (i.e., primary and secondary use and chemistry), power consumption and longevity. This information is analysed to show the course of design decisions adopted by industry and identifying opportunity for further innovation. We identify fundamental limits in power consumption, longevity and size as well as the interdependencies and trade-offs. We propose a figure of merit to quantify volumetric efficiency within specific therapeutic targets, battery technologies/capacities, charging capabilities and electrode count. Finally, we compare commercially available implantable medical devices with recently developed systems in the research community. We envisage this analysis to aid circuit and system designers in system optimisation and identifying innovation opportunities, particularly those related to low power circuit design techniques.

Index Terms—Neurostimulators, neuromodulation, implantable medical devices, neural interface, energy efficiency, miniaturisation, battery

I. INTRODUCTION

THE prevalence of neurological disorders (approximately 1 in 6 of the world's population) coupled with our improving understanding of disease mechanisms and advances in microtechnology have all driven a steady growth in implantable neurostimulator research and translational efforts. From chronic pain to Parkinson's disease (PD), the number of clinical applications being addressed using neurostimulation is ever increasing (Fig. 1). The neuromodulation market is expected to grow from USD 4.4 billion in 2018 to USD 11.3 billion by 2026 [1], evincing an important expectation for the impact of such research.

With the availability of such technology, what was once considered last resort will progressively become elective at earlier stages in disease treatment. An emerging trend has been the application of neurostimulation beyond drug-refractory diseases (e.g., PD or epilepsy) to conditions that have been traditionally addressable through pharmaceutical interventions. One approach here has been the application of bioelectronic medicines ('electroceuticals') [38], [39] to modulate the autonomic nervous system for immune-mediated inflammatory diseases, e.g., rheumatoid arthritis [40].

The progression of neurostimulation technology over the past two decades can be clearly observed in the increased output of the research community (Fig. 2), in addition to a more recent surge in translational activity within the neurotechnology and medical devices industry.

Despite this significant level of activity, the literature currently lacks a comprehensive review from a circuit and systems standpoint. Existing reviews are either focused on clinical outcomes (i.e., efficacy) [41], [42], [43], or specific technical components [44], [45], [46], [47], [48], but do not consider the entire device.

To the best of our knowledge, this is the first comprehensive review of state-of-the-art, commercially available neurostimulators. We analyse design parameters and performance metrics of 45 implantable medical devices aimed at six different neural targets.

More specifically, we studied the trade-off between battery capacity and device volume, as well as their relationships with battery chemistry. We then benchmark those devices alongside modern cardiac pacemakers that represent a more established market. In addition, we presented volumetric trends of neurostimulators over time. We broke down energy utilisation into different consumption sources. These results, along with our volumetric analysis, enabled us to estimate some miniaturisation limits for battery-powered neurostimulators given the current technologies of battery and connectors. We defined a Figure of Merit (FoM) based on the insights gained in the aforementioned analyses, and applied it to the assessed device set as well as some research platforms.

This work is organised as follows: Section II presents the device inclusion criteria considered for this review; section III presents an energy-flow model for a generic neurostimulator system and its application to the assessed devices; Section IV

Santiago Martínez is with the Electrical Engineering Department of the School of Engineering at Universidad de la República, Uruguay and is also with CCC Medical Devices, part of Integer Holdings Corporation (CRM and Neuromodulation) (e-mail: smartinez@fing.edu.uy).

Francisco Veirano is with the Electrical Engineering Department of the School of Engineering at Universidad de la República, Uruguay (e-mail: fveirano@fing.edu.uy).

Timothy G. Constandinou is with the Department of Electrical and Electronic Engineering at Imperial College London, UK and is also with the UK Dementia Research Institute (UKDRI), Care Research and Technology Centre (e-mail: t.constandinou@imperial.ac.uk).

Fernando Silveira is with the Electrical Engineering Department of the School of Engineering at Universidad de la República, Uruguay (e-mail: silveira@fing.edu.uy).
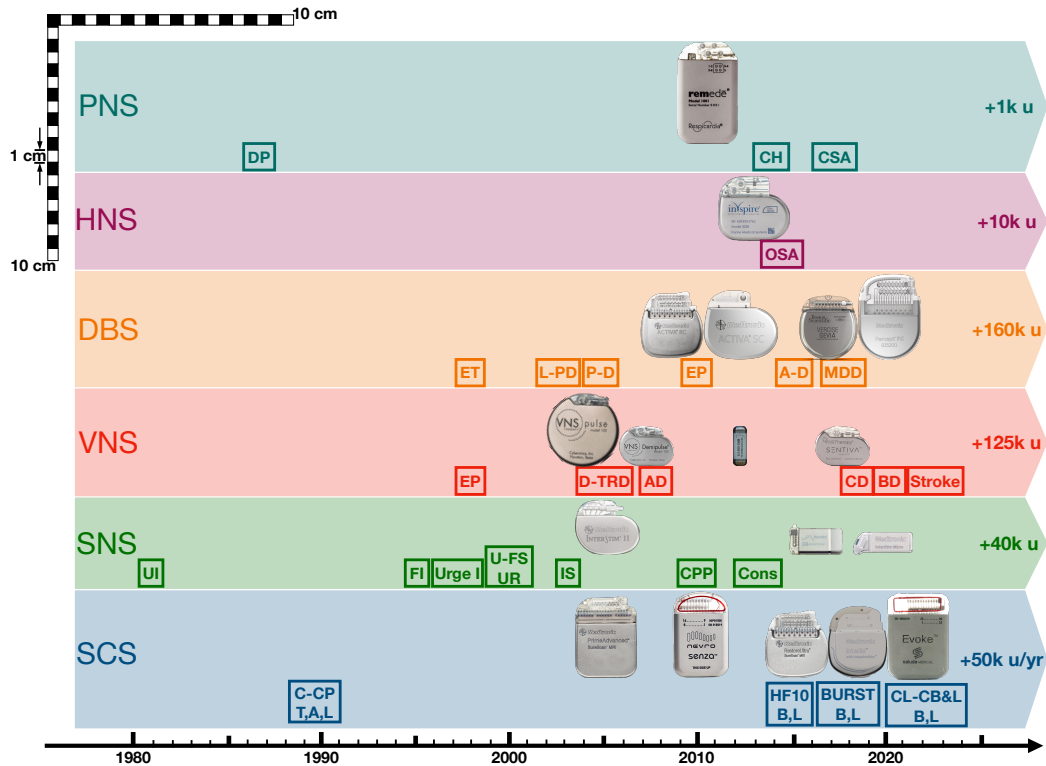
Fig. 1. Significant milestones in neurostimulation divided by neural target. Selected examples were illustrated to scale to convey the breadth across different form factors of current technology. In addition, reported patient number per target was included (absolute figures except for SCS, presented as patient number per year). **PNS** DP: Diaphragm pacing; CH: Chronic hypoventilation; CSA: Central sleep apnea; ([2], [3], [4])- **HNS** OSA: Obstructive sleep apnea; ([5], [6], [7]) - **DBS** ET: Essential tremor; L-PD: Levodopa-responsive Parkinson's disease; P-D: intractable (drug refractory) primary dystonia; EP: Epilepsy; A-D: Alzheimer's dementia; MDD: Mayor depressive disorder; ([8], [9], [10], [11], [12]) - **VNS** D-TDR: Difficult to treat depression; AD: treatment-resistant anxiety disorder; CD: Crohn's disease; BD: Rapid cycling bipolar disorder; Stroke: Stroke; ([13], [14], [15], [16], [17], [18], [19]) - **SNS** UI: Urinary urge incontinence and non-obstructive urinary retention; FI: Faecal incontinence; Urge I: Urgent incontinence; U-FS UR: Urgency-frequency syndrome and urinary retention; IS: interstitial cystitis; CPP: Chronic pelvic pain; Cons: Constipation; ([20], [21], [22], [23], [24], [25], [26]) - **SCS** C-CP T,A,L: Chronic pain from nerve damage in the trunk, arms or legs; HF10 B,L: High frequency spinal cord stimulation for chronic pain in low back or legs; BURST B,L: Burst spinal cord stimulation; CL-CB&L B,L: Closed-loop spinal cord stimulation for chronic back and leg pain ([27], [28], [29], [30], [31], [32], [33], [34], [35], [36], [37]).
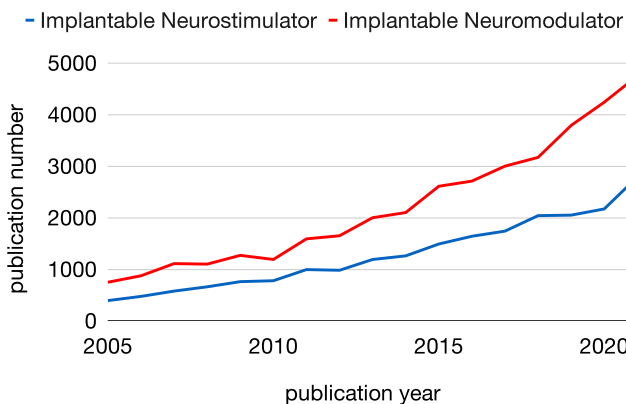

Fig. 2. Publication number obtained from Google Scholar for the key words "Implantable Neurostimulator" and "Implantable Neuromodulator" since 2005.

presents the relationship between total device volume and battery capacity and chemistry; Section V presents device miniaturisation limits; Section VI presents an overall comparison including some perspectives from the research domain;

and finally, Section VII, concludes this review.

II. SCOPE: DEVICES AND THERAPIES

A. Implantable neural device classification

Implantable devices which interact with the nervous system can be classified in three categories: open-loop neurostimulators, closed-loop neurostimulators and neural monitors (also including brain computer interfaces).

Open-loop is currently the most widely adopted paradigm in implantable neurostimulation devices. It consists on the delivery of a stimulation therapy determined by a set of predefined parameters. Stimulation waveform and sites are programmed by a physician according to patient needs.

On the other hand, closed-loop approaches enable systems to stimulate in response to neural activity. In closed-loop systems, neural signals are monitored and therapy is adjust according to this information (i.e. detected biomarkers). Closed-loop paradigms improve open-loop systems by responding directly to patient state providing an on-demand, adaptive therapy [39], [49], [50], [51], [52].

Some examples of closed-loop approaches involve the utilisation of evoked compound action potential (ECAP) to

determine the efficacy of spinal cord stimulation [53], the detection of overactivation of the intercostal muscle to determine ventilation effort in the treatment of obstructive sleep apnea by hypoglossal nerve stimulation [54], and the measure of breathing patterns in phrenic nerve stimulation to treat central sleep apnea [55]. In spite of the good prospect of this approach, continuous stimulation and recording bares great challenges. Stimulation floods the electrode-tissue interface with charge, producing substantial artefacts in recorded neural data. Several strategies has been proposed to reject artefacts at both front-end (analogue) and back-end (digital) [56]. Closed-loop platforms is a domain of intense current research. Some interesting reviews on commercial and research closed-loop neuromodulators can be found in [51], [52]. One of the most recent developments is the AlphaDBS [57] which is a commercial DBS device to treat Parkinson's disease. It has already gained the CE mark for its traditional (i.e., open-loop) therapy, and the effectiveness of its adaptive (i.e., closed-loop) therapy is currently under evaluation through clinical trials [58].

It is worth to mention that, during follow-ups, physicians adjust the device stimulation parameters according to patient needs. Additionally, some systems also implement a patient-in-the-loop strategy by giving the user a patient controller to adjust the therapy among a set of predefined programmes predefined by a physician. Those factors contribute to create a feedback loop even if the patient is utilising an open-loop neurostimulator.

Neural monitors only have sensing capabilities. These devices are intended to record neural activity in order to understand patient's neural behaviour. One iconic example are the brain computer interfaces (BCI) which record brain activity (e.g., cortical signals) in order to translate this into actionable information whereby, for instance, an amputee can control an artificial limb [59], [60]. Another interesting platform is the neural dust [61], which is a tiny, ultrasound-powered sensor intended to measure neural activity of any kind.

A conceptual block diagram for implantable neural devices is presented in Fig. 3. It is divided into battery, output connectors, and the electronic circuit.
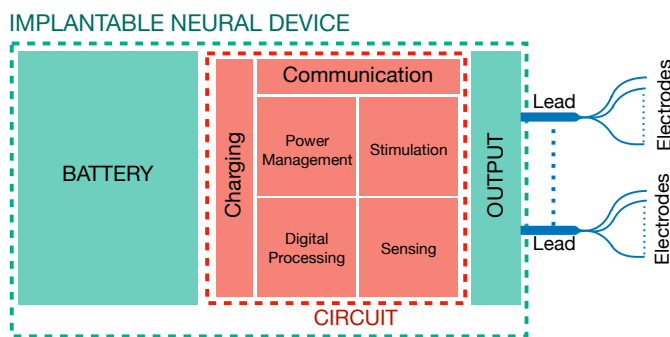

Fig. 3. Conceptual block diagram of an implantable, battery-powered neural device.

The circuit contains sub-modules aimed at: stimulating the neural tissue (stimulation), recording biological signals (sensing), communicating to/from the outside through RF to receive commands and send records (communication), digital processing to command stimulation, sensing and telemetry (digital processing), power management to supply these modules (power management), and charging (charging).

The scope of this study covers fully implantable, battery-powered and commercially available neural platforms with stimulation capabilities (as depicted in Fig. 4). These criteria exclude an important type of neural stimulator as cochlear implants, since these systems have a distributed architecture with an internal part that stimulates the cochlea and an external part comprising the microphone, a speech processor and the system battery. For benchmarking purposes, state-of-the-art pacemakers as well as research platforms were included. The rest of this section describes the neural targets addressed by the investigated devices.
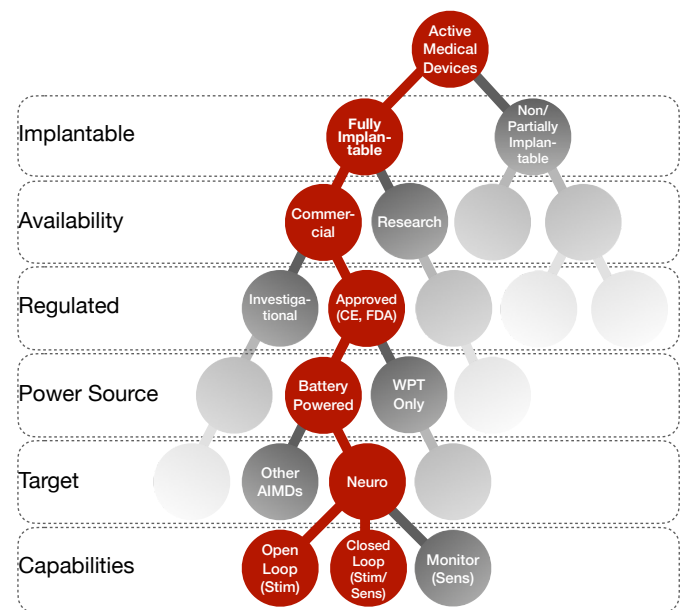

Fig. 4. Inclusion criteria for our review.

B. Neural targets

The vagus nerve is the cranial nerve that connects the brain to all the major organs in the body, and is associated with controlling autonomic responses. Implantable vagus nerve stimulators (VNS) has been used to modulate the immune system to alleviate rheumatoid arthritis, treat heart failures, prevent epileptic seizures, and treat stroke, among others.

Spinal cord stimulators (SCS) are typically intended to stimulate the spinal cord for the treatment of chronic pain. Classical SCS are based on a principle named 'gate control theory of pain' [62]. Upon an injury, pain signals are transmitted to the brain through the spinal cord. Melzack and Wall suggested there is a way to block this transmission by stimulating certain "gates" at the dorsal horn, inhibiting painful sensation.

Deep brain stimulators (DBS) has been used for treatment of different neurological diseases like Parkinson, epilepsy, dystonia, essential tremor, etc. [63]. A special case of DBS,

is the brain-responsive stimulation intended to treat epilepsy operating in closed loop. This will be denoted as RNS.

Sacral nerve stimulators (SNS) stimulates the sacral nerve in order to restore the neural communication between the bladder or bowel and the brain to avoid incontinence.

Phrenic nerve stimulators (PNS) sends electric pulses to the phrenic nerves in order to address central sleep apnea (CSA). CSA is a serious disorder caused by intermittent interruption of neural signals from the respiratory control centre. This affects the normal breathing pattern during sleep. It impacts negatively on life quality and health. By means of a sensing lead, PNS can detect an anomalous breathing pattern and deliver stimulation pulses to the phrenic nerves to contract diaphragm muscles to assist and reinforce robust breathing.

Hypoglossal nerve stimulators (HNS) are another kind of devices intended to treat apneas. In this case, a sense lead detects overactivation of intercostal muscle (which is indicative of inspiration difficulties). Upon detection, the HNS stimulates the hypoglossal nerve to open the airway.

C. Investigational platforms

An active area of bioelectronic medicine is focused on developing investigational platforms. These systems intend to be tools whereby we can gain a better understanding about the nervous system and its disorders. Investigational devices are capable of recording what is deemed meaningful neural activity, typically related to an abnormal electrical state and also to the activity during electrical neuromodulation. The ultimate end of this effort is to achieve new or refined methods and treatments, yielding optimal clinical outputs. Some exemplary systems, representative of the state-of-the-art are [64], [65], [66], [67], [68], [69], [70]. Three of them that present enough data to analyse them as done in this study are compared to commercially available neurostimulators in Section VI-C.

III. ENERGY CONSUMPTION

In battery-powered devices, energy consumption is a critical aspect. It impacts time between recharges (in case of rechargeable platforms) and device longevity. These factors affect the patient burden due to frequent recharging procedures or need for device replacement. Among all sources of energy consumption, the stimulation circuit accounts for an important fraction of the total consumed energy. Particularly, the amount of energy intended to stimulate the neural tissue has been shown, as expected, to be correlated with battery life in deep brain stimulators [71], [72].

In the rest of this section we present the typical neurostimulation waveform and a generic circuit architecture which is capable of delivering this kind of therapy. As we discuss later, regarding energy losses, the results of the analysis for this architecture are also applicable to other common variants. Based on the proposed circuit, and consumption and longevity data provided by device manufacturers, we calculate the amount of energy directed to the neural tissue. In order to assess the room for improvement in the circuits and system design, we consider some hypotheses about power management efficiency and losses of the stimulation circuit. Those hypotheses are supported by published results. The resulting analysis breaks down the energy that is not directed to the neural tissue between losses and internal consumption for each commercial device. Our aim is helping circuit and system designers to gain a better understanding about the consumption sources of commercial neurostimulators and which aspects look promising research lines.

The mechanisms whereby neurostimulators deliver energy to the target tissue can be divided between voltage and current stimulation. Constant-current stimulation (CCS) allows for consistent charge delivery with independence of impedance fluctuations. This has been the most important stimulation mechanism among neurostimulators for the last 15 years.

Typical CCS therapy waveform is depicted in Fig. 5.a. It typically consists of rectangular stimulation pulses whose shape depend on current amplitude (I) and pulse width (PW). Depending on the system, these pulses can be followed by an active balance phase aimed at preventing charge build-up in the electrode-tissue interface. In case the active balance is not present, another balance phase is implemented that discharges the series decoupling capacitors (Fig 7) after a pre-defined number of stimulation pulses. We will only consider these two traditional balancing strategies. More recently, other techniques to ensure electrode and tissue integrity have been proposed. These take into account a more complete model of the electrochemical operation of the electrode-tissue interface [73], [74], [75] and in some cases may not use decoupling capacitors.

This pulse sequence (i.e., stimulation pulse and active balance pulse) is repeated periodically (with a period given by T) while stimulation is in course. Additionally, some therapies implement a duty cycle (δ as in Fig. 5.b) by switching from active to inactive stimulation for a programmable amount of time.
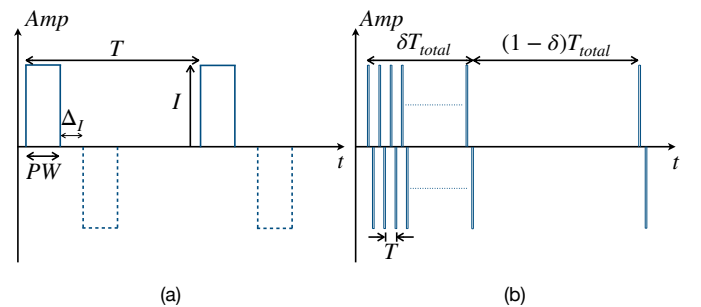

Fig. 5. Stimulation waveform for CCS therapy. It typically consists on a periodic square pulse (left) which can be followed by an active balance pulse (dashed pulse). Additionally, therapy can switch from active to inactive and vice versa (right), complying with a programmable duty cycle.

There are two traditional topologies for CCS output stage (see Fig. 6) [76]: a) current source and current sink electrode driver [77], [78], [79], [66], and b) single source and switching H-bridge [80], [81]. In the first case (Fig. 6.(a)), the charge injection/absorption to/from the electrode is implemented with a dual structure consisting of a current source and a current sink. In order to deliver current to the tissue, one electrode is
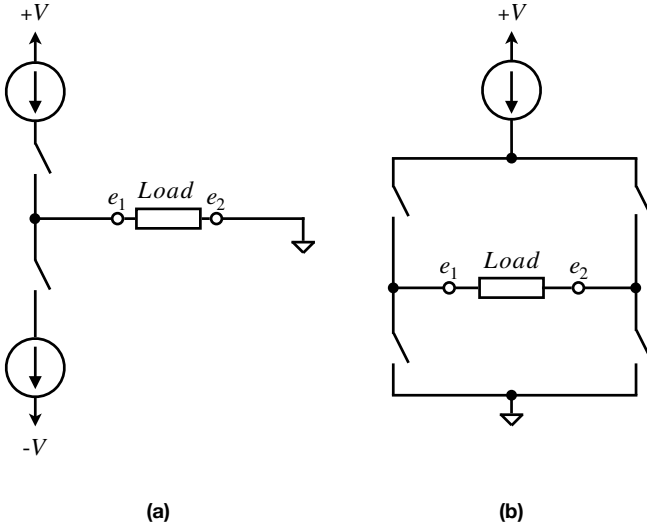
(a) **(b)**

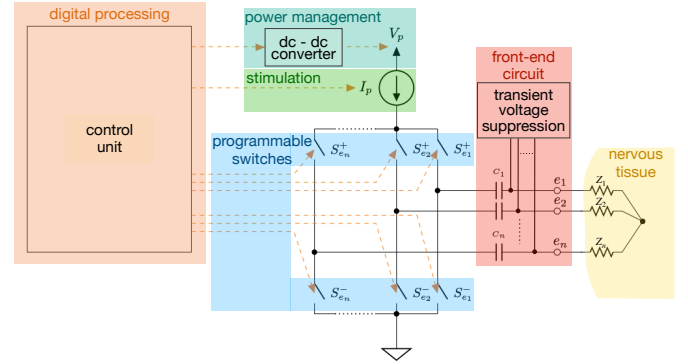Fig. 6. Traditional stimulation topologies intended to implement CCS.

Fig. 7. Model of a neurostimulator circuit capable of producing CCS therapy. It contains all the required hardware to deliver the corresponding stimulation pulses as well as some protection measures.

connected to a reference voltage, ideally at the midpoint of the voltage rails. A good matching between both current source and current sink as well as calibration is typically required to obtain a proper charge balance. These kind of structures are advantageous when the electrode count is high, since the switch quantity increases linearly with the electrode number. The second case (Fig. 6.(b)) requires only a single current source (or sink) which is in charge of the active and active balance phase. This is possible thanks to a switching H-bridge which connects the source with the electrodes. This structure simplifies the charge balance, but requires a greater number of switches, becoming a recommendable topology for devices with reduced electrode number. A detailed review concerning different solutions to implement stimulation interfaces can be found in [82].

Circuit implementation details of commercial neurostimulators is not publicly disclosed. Therefore it is not possible to know which implementation each manufacturer adopted. Nonetheless, as discussed next, the analysis performed regarding energy efficiency applies to both architectures in Fig. 6 and others derived from those.

Fig. 7 presents a generic stimulation circuit which is capable of delivering the aforementioned CCS stimulation waveform. It is composed of several sub-systems: stimulation source, power management, programmable switches (H-bridge), front-end, and control unit. It is worth mentioning that even though this circuit has the topology of (Fig. 6.(b)), the results here presented regarding energy consumption will be applicable for the topology of (Fig. 6.(a)). This will be further analysed when appropriate.

The stimulation source I_P is in charge of injecting and absorbing charge to and from the electrodes. The array of programmable switches channels the current flow to the selected (i.e., programmed) electrodes. With this topology, each electrode can be utilised as current source ($S_{e_i}^+$ closed) or sink ($S_{e_j}^-$ closed) independently. It is worth mentioning that one of

those electrodes could be the device case.

Front-end circuit consists on a series of decoupling capacitors that help to assure that the average current directed to the tissue will be null. In addition, the front-end contains an array of transient voltage suppressors aimed at protecting the device from being damaged by high voltages due to external defibrillators, high power electrical fields applied to the patient (particularly, during medical treatments) or electromagnetic non-ionizing radiation. All those factors are considered in international standards such as BS EN 45502-1, ISO 14708-3 and ISO 14708-1 [83], [84], [85].

The power management module (i.e., dc-dc converter) sets a programmable voltage source V_P which in turn feeds the entire stimulation circuit. Its programmability allows the source to be adjusted in real time in response to voltage fluctuations at the stimulation electrodes due to impedance changes, keeping the stimulation current source with the necessary voltage headroom and minimising its power losses as well. An example of this strategy is presented in [86].

A control unit drives the entire stimulation circuit by setting the target voltage at the dc-dc converter outlet, selecting the stimulation current, and driving the corresponding programmable switches according to the waveform timing and shape. Additionally, this control unit can perform another activities such as digital processing of recorded data, telemetry, and other tasks related to standards compliance [87], [88] like risk control mechanisms, integrity checks, housekeeping, etc.

A Sankey (energy-flow) diagram for an entire neurostimulator system is presented in Fig. 8 considering all typical sources of energy consumption.

In order to characterise the energy invested in stimulating the nervous system, a single figure termed Total Electrical Energy Delivered (TEED) was created [89], [90]. First presented for DBS, it was spread for all other neurostimulation platforms and it is utilised as a measure of the amount of energy delivered to the neural tissue [91], [92], [72], [93], [94].

It is essentially the amount of energy directed to the electrodes in 1 second:

$$\text{TEED} = Z \times I^2 \times PW \times 1/T \times 1 \text{ s}. \tag{1}$$
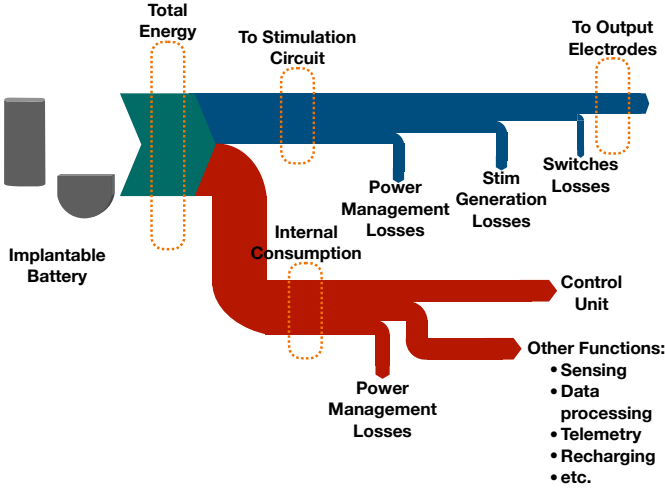
Fig. 8. Sankey (energy-flow) diagram for a generic battery-powered neurostimulator. The energy stored in the battery is consumed by the stimulation circuit and in internal activities. Flow thicknesses are only representative of typical energy share of each consumption source.
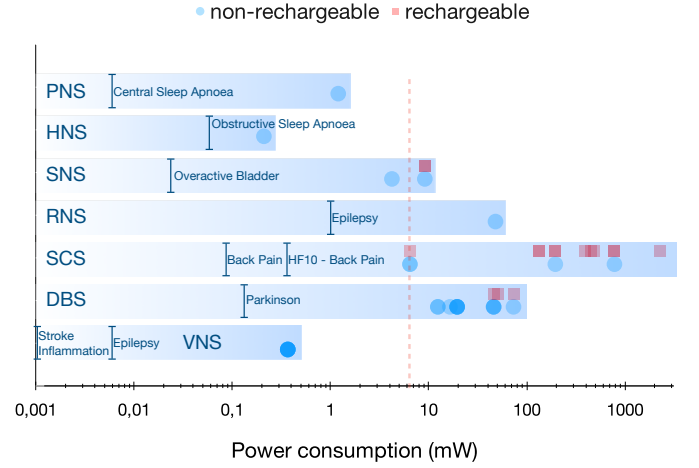

Fig. 9. Neurostimulation therapies and their maximum average stimulation power along with the average power to effectively treat some conditions. All surveyed rechargeable devices present maximums greater than 5 mW which can be understood as a practical threshold for manufacturers decision in terms of battery chemistry.

Where Z is the impedance between the positive electrodes (those programmed as source) and the negative electrodes (those programmed as sink). It is worth mentioning that the consensus, standardised way to model the load of a neurostimulator is established in standard ISO 14708-3, subclause 6.101 as a resistor [84]. This is also the practice used by manufacturers to report specifications concerning device longevity. Such standard states that a more complex impedance may be considered if required, but this is usually not applied for energy consumption analysis. The rest of the parameters are those depicted in Fig. 5.

Neural targets require different energetic levels, so the programmable values I, PW and T depend on the device intended use. In Fig. 9, the maximum average stimulation power for each of the assessed therapies is presented. It was computed as the TEED per second, using the maximum programmable amplitude and pulse width, and the minimum period. In addition, the average power reported in several trials aimed at showing therapy effectiveness (refer to Table II) was included. This figure offers some insights about the required power to effectively stimulate by means of electricity some specific regions of the neural system.

The TEED can also be utilised to obtain the total amount of energy delivered to the electrodes over the time span from a fully charged battery state to its complete depletion (T_{batt}), as follows:

$$E_{out} = \texttt{TEED} \times (1 + \gamma) \times T_{batt} \times \delta, \qquad (2)$$

where γ is a binary variable which is "1" if the stimulation presents an active balance and "0" otherwise. Time T_{batt} can be understood as the time between recharges, in case of rechargeable platforms, or the device longevity (for non-rechargeable ones).

Device manuals often contain information regarding device longevity or time between recharges for a given parameter set and electrode-tissue impedance. For the assessed devices,

this information can be found in Table IV, under column 'Consumption' which presents the reported longevity and the parameters value at which the test was conducted. In order to breakdown the remaining energy into other consumption sources, some considerations were taken, as follows:

- the energy drawn by the programmable switches has a negligible effect on device longevity, since its on resistance normally is far lower than the electrode-tissue impedance.
- some device features are disabled or not utilised when computing battery duration to provide longevity estimations. Some of those features are telemetry, data processing, recharging and sensing.

Those considerations narrow the consumption sources to, from the stimulation circuit point of view, power management and stimuli generation losses and, from the internal point of view, to power management losses and control unit.

Energy losses in the stimulation circuit depend on the voltage headroom (V_H) of the current source. Considering this voltage as constant, the losses can be computed as:

$$E_{Stim}^{Losses} = I \times V_H \times PW \times 1/T \times (1 + \gamma) \times T_{batt} \times \delta. \quad (3)$$

Having estimated the total energy drawn from the dc-dc outlet, total energy of the stimulation circuit can be calculated considering the power efficiency of the converter η_{dc-dc}:

$$E_{Stim}^{Total} = \frac{E_{out} + E_{Stim}^{Losses}}{\eta_{dc-dc}}. \qquad (4)$$

As it was previously noted, this result is independent from the topology selected for the stimulation circuit (refer to Fig. 6), since E_{out} depends only on the stimulation waveform, and E_{Stim}^{Losses} depends on the corresponding voltage headroom of the current source which is actually delivering charge (in case of a dual source topology, both sources are almost identical and the losses in both phases are equal).

The remainder energy will be consumed internally:

$$E_{Internal} = E_{Batt}^{Total} - E_{Stim}^{Total}. \qquad (5)$$

To determine those factors, we considered the following hypothesis:

- the voltage headroom V_H is constant and has a value of $1.2\,V$ for any stimulation current and any electrode impedance while the device is injecting or absorbing charge to its electrodes.
- the dc-dc converter power efficiency (η_{dc-dc}) was set at $90\,\%$.

We consider this selection as a best case scenario, since even though the voltage headroom can be considered slightly high for state-of-the-art stimulation current sources (which have been reported varying from 150 mV to 1.8 V [77], [78], [79], [66], [80], [81]), the fact that this is constant implies, as it was mentioned before, that there is a control that keeps track of the electrode voltage and adjust the dc-dc outlet accordingly to assure V_H. In addition, the efficiency of the power management circuit was selected higher than the state-of-the-art dc-dc converters found in biomedical applications, which varies from 30 % up to 86 % [95], [96], [97], [98], [99], [100], [101]. The energy consumption breakdown for each assessed device is presented in Fig. 10. These results show that the amount of energy devoted to stimulate the neural tissue accounts for less than 25 % of total energy budget whereas up to 20 % are losses in the stimulation circuit and more than 50 % is consumed in internal activities (e.g., digital processing, telemetry, integrity checks, etc.). It is noteworthy that even though internal consumption and stimulation circuit losses depend on the selected values of voltage headroom (V_H) and dc-dc efficiency (η_{dc-dc}), the energy directed to the tissue, E_{out}, is directly computed with data provided by manufacturers in device manuals and because of that it is independent from any assumption regarding device architecture, power management and circuit efficiency. Changing V_H or η_{dc-dc} does not change the total energy amount not invested in stimulating the neural tissue, and only has an impact on how this energy is subdivided between stimulation circuit losses and internal activities. Selecting other values for those parameters will only change mildly the results seen in this study.

To represent the share of each consumption source with respect to the total energy available, we considered E_{Batt}^{Total} independent from discharge rate and charge/discharge cycle number when applicable. In practice, these operating conditions tend to reduce total available energy, introducing an error in our estimations. Absolute values of E_{out}, E_{Stim}^{Losses} and total stimulation energy remain unchanged, but, since internal consumption is computed as the difference between the energy stored in the battery and the energy drawn by the stimulation circuit, these is overestimated. The low/medium therapy consumption, along with the high internal consumption, has to be evaluated with careful consideration, since this is not necessarily indicative of an inefficient solution. A particular case is closed-loop devices. In closed-loop neurostimulators, an increased complexity and energy consumption non-directed-to-the-tissue is required to assure a more effective stimulation by adjusting the stimulation waveform and/or providing the therapy only when required. One example of this is the NeuroPace RNS [102], which continuously monitors brain activity looking for unusual electrical activity which might indicate the advent of a seizure (therapy is only delivered when this happens). Continuous monitoring and detection naturally impact dramatically on internal consumption, rendering this the most important factor among all consumption sources. Nevertheless, we believe that our goal as designers is to be able to provide the same functionality with less power consumption, maximising the energy directed to the neural tissue. With those considerations, we understand there is plenty of room for improvement in digital power processing as well as stimulation circuit efficiency.

IV. BATTERIES AND VOLUME

In this section we study volumetric characteristics of commercially available devices. In particular, we investigate miniaturisation trends over time and how the overall device volume is affected by the selected battery (i.e., its capacity and chemistry) and device electrode count.

A. Batteries

Batteries can be divided in two groups, depending on their ability to be recharged.

Primary batteries are non-rechargeable and have to be discarded when discharged. In the context of implantable devices, this implies that the device has to be explanted and replaced. Primary battery based devices are simpler since they do not require any charging management.

On the other hand, secondary batteries are rechargeable. This allows an implantable device to extend its life longer than its battery duration. Secondary batteries usually have lower energy densities and poorer charge retention than primary batteries. In addition, implantable devices require a greater complexity to adopt rechargeable batteries, from the necessity of a charging coil to an additional circuit aimed at charging management. In spite of these implementation difficulties, the flexibility granted by rechargeability can be highly desirable, since different consumption levels can be absorbed by changes in recharge frequency while keeping the device operative for long time. In this case, replacement is required when the number of charge cycles is close to reach the maximum specified by the battery employed.

Lithium metal has been the most important anode material to construct both primary and secondary batteries in recent decades. It offers several advantages such as high voltage, high energy density, and good shelf life, among others. An interesting review of the state-of-the-art of implantable batteries can be found in [103]. Primary battery chemistries found in this assessment are lithium-carbon monofluoride (Li/CFx), lithium-carbon monofluoride silver vanadium oxide (Li/CFx-SVO), lithium-iodine (Li-I2), and, as secondary chemistry, lithium-ion (Li-Ion).
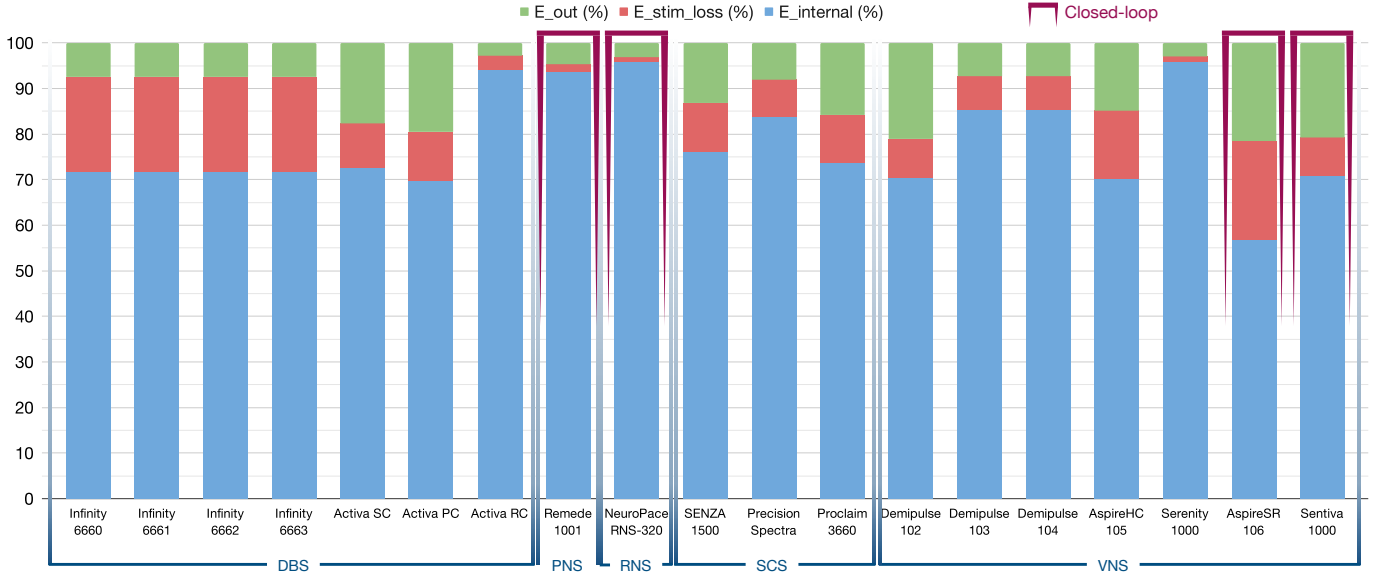
Fig. 10. Energy consumption breakdown. With a constant voltage headroom V_H of 1.2 V and a dc-dc efficiency η_{dc-dc} of 90 %, the aggregate amount of stimulation losses (power management losses and stimuli generation losses) accounts for up to 20 % of total energy budget. Less than 25 % of the total energy is delivered to the neural tissue whereas more than 50 % is spent in internal activities.

B. Trends in volumetric energy density

In order to understand the impact of battery technology on neurostimulation platforms, the relationship between battery capacity and device volume was assessed and presented in Fig. 11. In addition, several state-of-the-art cardiac pacemakers were included in this assessment. Cardiac pacemakers are a well known kind of device with several decades of evolution. This "well polished" technology is a sound benchmark to evaluate the current state of neurostimulators, which in some cases are so novel that only one device is available to stimulate some neural target. Naturally, cardiac pacemakers and neurostimulators are not directly comparable, since they differ in stimulation mode (i.e., voltage mode for pacemakers versus voltage or current mode for neurostimulators) and in several operational aspects. Nonetheless, cardiac pacemakers provide a standard for energy-volume trade-off for active implantable medical devices.

As it can be noticed in Fig. 11, battery chemistry is a determinant factor in defining overall device volume. For each chemistry, devices tend to group along a straight line in the [volume, capacity] plane (presented in the figure as dashed lines). This defines a volumetric energy density for the overall platform as presented in Table I labelled as 'device trend'.

TABLE I
TRENDS IN VOLUMETRIC ENERGY DENSITY FOR IMPLANTABLE
NEUROSTIMULATORS.
V: NOMINAL VOLTAGE.
σ: THEORETICAL VOLUMETRIC ENERGY DENSITY.

Chemistry	V	σ	Device trend	Ratio
Li-Ion [104]	4.1 V	98 mAh/cm^3	12 mAh/cm^3	13 %
Li-I2 [104]	2.8 V	321 mAh/cm^3	47 mAh/cm^3	15 %
Li/CFx [104]	3.0 V	212 mAh/cm^3	50 mAh/cm^3	24 %
Li/CFx-SVO [105]	3.0 V	333 mAh/cm^3	215 mAh/cm^3	65 %

Rechargeable neurostimulators (based on Li-Ion chemistry) offer the smallest volumes (i.e., SetPoint and Axonix), yet they present the poorest energy/volume relationship. On the other hand, non-rechargeable, Li/CFx-SVO chemistry based neurostimulators, have the highest energy density.

In order to gain a better understanding about the trade-off between volume reduction and energy capacity, we compared those results against the practical energetic limits for each battery technology. Actual capacity available of commercial batteries depend not only on the theoretical density achieved by the specific chemistry but also on structural characteristics, in particular, the required amount of non-energy-producing materials. As a result, actual capacity available is between 20 % and 30 % lower than the theoretical value [104]. This means that actual volumetric energy density (σ_E) can be estimated based on the theoretical volumetric energy density (σ) and an empirical penalty factor (κ), which varies from 0.20 to 0.30, as follows:

$$\sigma_{E_{\{Min,\ Max\}}} = (1 - \kappa_{\{Max,\ Min\}})\sigma. \tag{6}$$

This defines a sector in the [volume, capacity] plane. For each battery chemistry, those sectors were superimposed over the empirical results and presented also in Fig. 11.

It is possible to appreciate that pacemakers, being a mature kind of implantable device, present a more efficient volume utilisation. In particular, Micra AV device [106] is very close to the practical limit given by its battery chemistry. This strongly depends on the absence of leads which reduce overall volume dramatically in small devices (please refer to Section V for further information about output connector and battery volume).
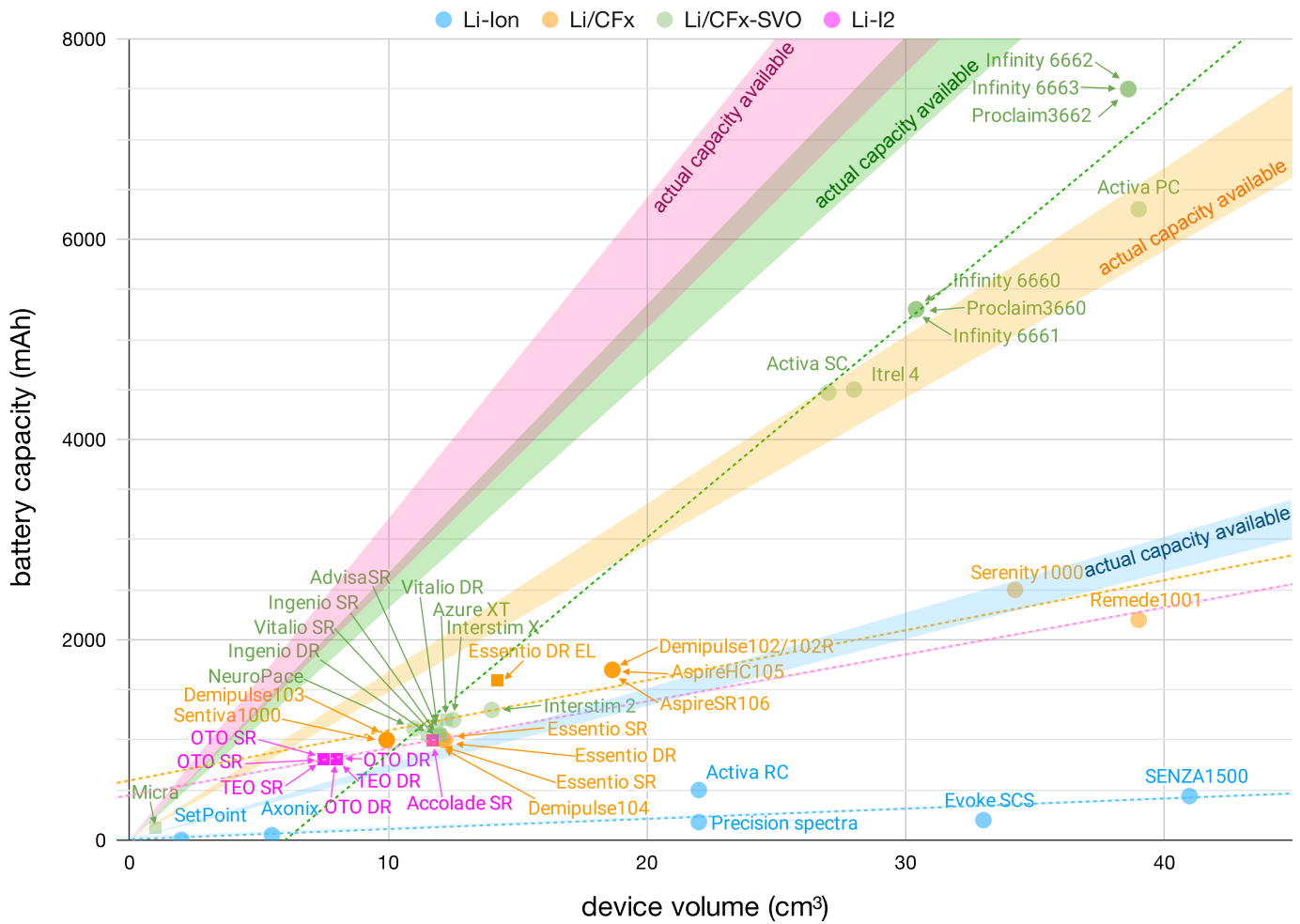
Fig. 11. Relationship between battery capacity and device volume. For each battery technology, devices tend to group along a straight line (as dashed) which defines an overall device volumetric energy density. Coloured sectors defines practical limits for each battery technology. Those were defined according to the theoretical volumetric energy density given by the battery chemistry and an empirical penalty factor, varying from -20% to -30%, observed in battery construction intended for medical devices. Circles represent neurostimulators whereas squares represent cardiac pacemakers, which are presented to compare neurostimulators state-of-the-art against a mature kind of implantable device.

C. Volumetric trends

Stimulation circuit as well as output connectors volume strongly depend on electrode number. As electrode count increases, the complexity of the stimulation circuit increases as well. This is due to the fact that the circuit has to direct the stimulation current through a greater combination of electrodes. Likewise, the size of the front-end circuit increases as well. Both factors contribute to obtain a greater stimulation circuit volume. Electrode number defines the number of contacts the output connector will require and, consequently, its volume.

Since electrode number depends on device intended therapy (see Fig. 12), its impact on circuit and output connectors renders overall device volume dependent on device intended use. To take this into account and allow fair cross-therapy comparisons, we assessed device volume for each platform and normalised it over the corresponding electrode number.

The normalised neurostimulator volume trends over time is presented in Fig. 13.

There is a clear miniaturisation tendency across all neu-
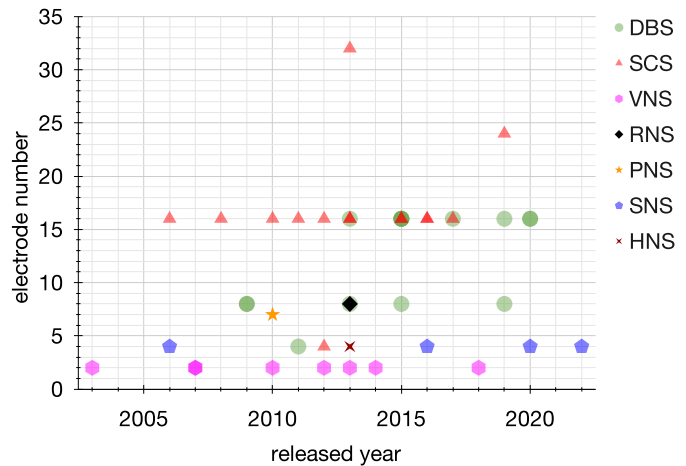
Fig. 12. Evolution of electrode number vs. device release year (i.e., received FDA PMA approval or CE mark).
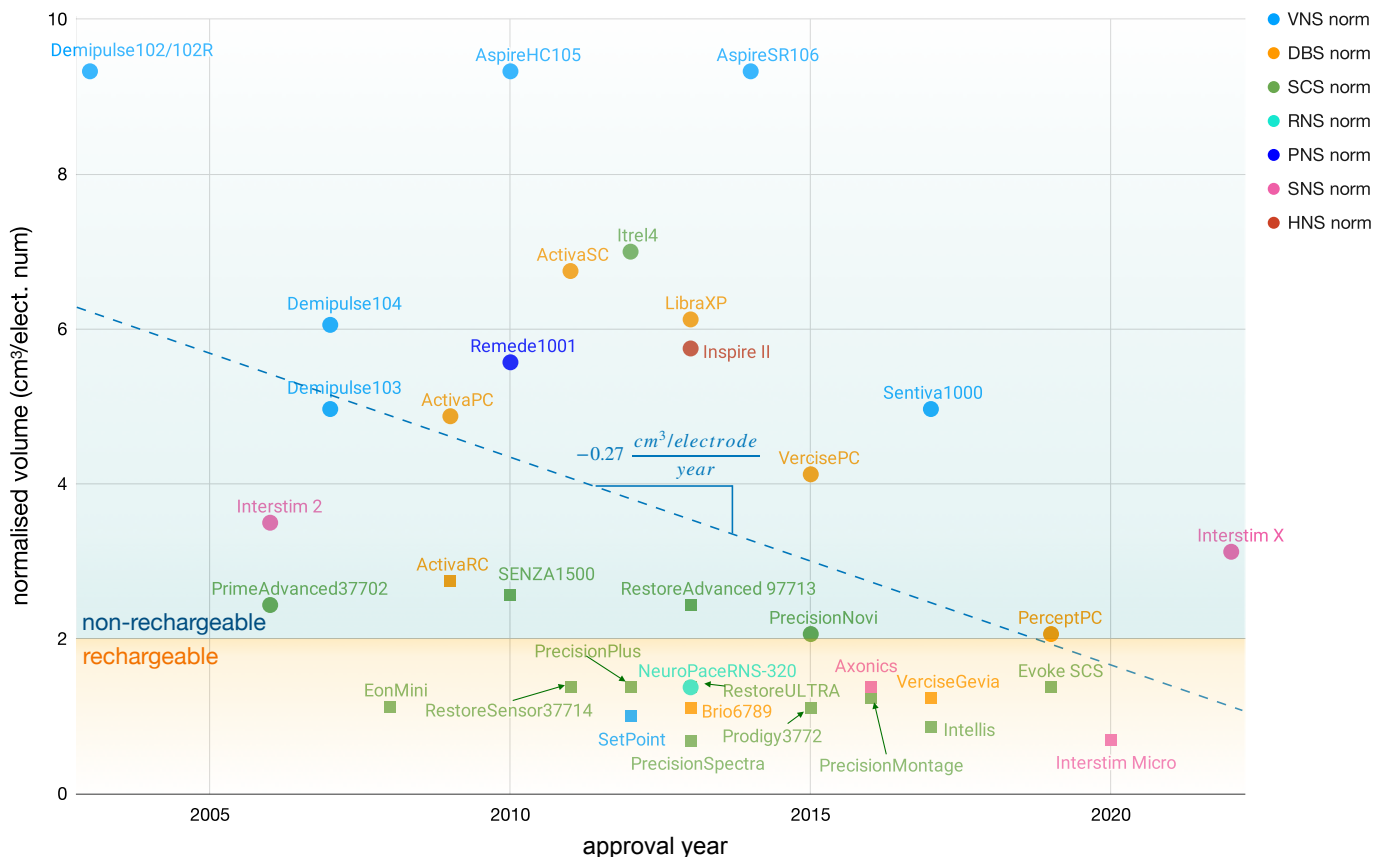
Fig. 13. Normalised device volume over device released year (i.e., received FDA PMA approval or CE mark). Volume normalisation, which is obtained by dividing total volume over electrode number, is conducted to fairly compare devices with different electrode number (being this an important factor in device volume). Colours indicate device therapy whereas shapes differentiate rechargeable (square) from non-rechargeable (circle) platforms. Over the last 15 years, there has been a neurostimulation volume reduction trend of $0.27\,\text{cm}^3$/electrode per year. The smallest figures are achieved by rechargeable platforms which present volumes lower than $2\,\text{cm}^3$/electrode.

rostimulation therapies which yields a volume reduction trend of $0.27\,\text{cm}^3$/electrode per year. This fact can be explained by a sustained reduction trend in non-rechargeable platforms and a growing use of rechargeable devices, which offer volumes lower than $2\,\text{cm}^3$/electrode.

Smaller implantable devices carry several benefits. They can improve patient satisfaction by their reduced volume and weight. Besides, volume reduction implies small packaging (typically titanium-based), which may reduce fabrication costs (since medical-grade titanium cases are one of the most expensive components in AIMD fabrication). Additionally, small form-factors enable other non-traditional methods to implant devices, such as through injection [107]. Considering Fig. 11 and 13, it seems clear that manufacturers leverage secondary cells to develop smaller devices by reducing battery volume.

V. PRACTICAL MINIATURISATION LIMITS

In this section practical miniaturisation limits for battery-powered neurostimulators are presented. Those are reckoned based on some suppositions about device energetic efficiency as well as battery and output connectors volume estimations.

A. Hypothesis

There is a fast and constant miniaturisation trend and energy efficiency improvement in electronics circuits that is not followed at the same pace by battery technology nor by connector technology. Therefore, when envisioning a practical limit for overall device miniaturisation, we expect it to come from these two last technologies. Thus, in the limit, we consider an ideal neurostimulator with the following characteristics:

- the entire circuit (please refer to Fig. 3) has a negligible impact on device overall volume.
- all available energy is directed to the electrodes.

The aforementioned features imply that the device form-factor is defined by battery and output connectors. Additionally, power losses in the stimulation circuit as well as internal consumption (e.g., digital processing consumption) are insignificant.

B. Battery volume

Taking into consideration the theoretical and practical considerations about volumetric energy density of batteries mentioned in Section IV, battery volume Vol_{batt} can be calculated as:

$$Vol_{batt} = \frac{c}{(1-\kappa)\sigma}, \qquad (7)$$

where:

- c: is the battery capacity.
- σ: is the theoretical volumetric energy density.
- κ: is the penalty construction factor (0.20 - 0.30).

If stimulation is the only consumption source, battery energy (E_{batt}) is defined to comply with device longevity (for primary sourced devices) or time between recharges (in case of secondary sourced devices) T_{batt}, given the stimulation power consumption ω:

$$E_{batt} = Vc = \omega T_{batt}, \qquad (8)$$

Where V is the battery voltage, which depends on battery technology. Hence, the minimum battery volume can be computed as:

$$Vol_{batt} = \frac{\omega T_{batt}}{V[(1 - \kappa)\sigma]}. \qquad (9)$$

C. Output connector volume

There is no standard intended for neurostimulator output connectors, mainly because the relatively reduced patient number. Due to that fact, manufacturers need not look for connectors compatibility, rendering publicly technical specification scarce [47]. Mature and widely used implantable devices, as cardiac pacemakers, have very well known standard connectors (i.e., IS-1, IS-4, DF-1 and DF-4), stated in ISO 27186 [108].

To obtain a sound estimation of connector volumetric costs, we considered the specification for connectors IS-4, which is aimed at 4 low-voltage electrodes cardiac pacemakers. To determine the minimum achievable volume per electrode given this technology, we modelled the connector as a cylinder (Fig. 14), whose length is equal to the addition of the following lengths (as defined in the aforementioned standard): "chamfer zone", "lead connector body", "transition zone", and "lead connector pin". As for diameter, we took the one defined by the "grip zone". The result consists on a best case volume of $0.354\,\text{cm}^3$, which is $0.088\,\text{cm}^3$/electrode.
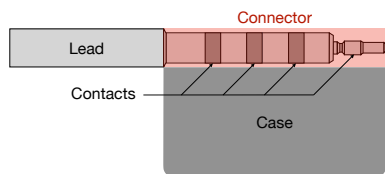
Fig. 14. IS-4 connector. In red, the estimated connector volume. Note this is a best case (i.e., minimum volume) since there are additional volumetric costs due to the size of the metallic contacts to assure a low resistance connection [47], [108].

The estimated connector volume Vol_{conn} can be obtained by the volumetric density computed before, as follows:

$$Vol_{conn} = \epsilon N_E, \qquad (10)$$

where:

- ϵ: is the output connector volume per electrode.
- N_E: is the electrode number.

TABLE II
AVERAGE POWER DIRECTED TO THE ELECTRODES.

Therapy	Ref	Amplitude	Frequency (Hz)	Pulse width (μs)	ω [1] (μW)
VNS - Epilepsy	[109]	1.5 mA	20	250	6 [2]
VNS - Stroke	[110]	0.8 mA	30	100	1 [2]
VNS - Inflammation	[111]	1.0 mA	10	250	1 [2]
SCS	[112]	3.6 mA	39.2	347	88 [2]
SCS HF10	[112]	1.6 mA	10 k	30	384 [2]
DBS - Parkinson	[113]	3.0 V	130	60	140 [2]
PNS	[114]	1.0 mA	40	300	6 [2]
HNS	[115]	3.0 V	33.9	94.3	58 [2]
SNS	[116]	2.0 V	14	210	24 [2]
RNS	[117]	12.0 mA	200	200	3000 [3]

[1] Considering an equivalent impedance of $500\,\Omega$ between positive and negative electrodes.
[2] Considering duty cycle equal to 100 %.
[3] Since feedback updates the parameter value set, the patient use profile defined as "High" (95th percentile) was considered.

D. Total volume

Under the mentioned suppositions, total device volume Vol_{total} can be estimated as:

$$Vol_{total} = Vol_{batt} + Vol_{conn} = \frac{\omega T_{batt}}{V[(1 - \kappa)\sigma]} + \epsilon N_E. \qquad (11)$$

This result depends on mechanical, technological and electrical characteristics as:

- State of battery technologies:
  - construction: κ.
  - chemistry: V and σ.
- State of connector technology:
  - volume per electrode: ϵ.
- Intended use:
  - stimulation power: ω (please refer to Fig. 9).
  - electrode number: N_E.
- Manufacturer decisions:
  - Battery duration: T_{batt}.

Therapy power depends on the actual parameter set, which is adjusted according to patient needs. In order to obtain a sensible therapy power, we considered parameter sets reported in trials aimed at showing therapy effectiveness, as in Table II.

Minimum device volume was estimated for several therapies in five different scenarios, comprising rechargeable and non-rechargeable battery chemistries as well as typical battery durations. Selected battery technologies were Li-Ion ($\sigma = 98\,\text{mAh/cm}^3$, V = 4.1 V) for rechargeable devices, and Li/CFx-SVO ($\sigma = 333\,\text{mAh/cm}^3$, V = 3.0 V) for non-rechargeable ones (which is the best technology reported in the surveyed neurostimulator data set). As for battery duration, we considered 1 day, 7 days, and 30 days for rechargeables and 1 year and 5 years for non-rechargeables. Typical electrode count was considered (obtained from Fig. 12). Penalty factor was selected in $\kappa = 0.25$. For each case, we computed the overall volume as well as the battery and output connectors volume on a percentage basis. The results are presented in Table III.

For rechargeable platforms, estimations show that overall device volume only depend on the output connector dimensions while its influence is limited in non-rechargeable devices, where battery volume plays an important role. These results

indicate that the smallest platforms are those with rechargeable batteries, and further miniaturisation depends on denser output connector technologies. The fact that device volume is independent from the battery bears one corollary which is applicable to non battery powered (i.e., wireless powered) platforms. This is that insofar as output connectors are not dense enough, wireless powered devices will not necessarily be smaller than their battery powered counterparts.

VI. OVERALL COMPARISON AND RESEARCH PERSPECTIVES

In order to characterise neurostimulation performance, a Figure of Merit (FoM) is proposed. This is aimed at comparing neurostimulators intended for any therapy with a single, common figure.

The FoM takes into consideration two factors, referred in Sections III and IV: energy efficiency and volume/electrode ratio. As it was mentioned, these numbers are indicative not only of a more efficient technology, but also they contribute to user satisfaction.

A. Energy efficiency factor

From the analysis conducted in Section III, the energy delivered to the tissue accounts for less than 25% of total available energy. A greater portion of the energy directed to the tissue will either increase device longevity or time between recharges, reducing patient burden due to device replacement or frequent battery recharge. For such a reason, we considered that an efficiency factor (F_{Eff}) is necessary to be included. That was defined as follows:

$$F_{Eff} = \frac{E_{out}}{E_{total}}, \tag{12}$$

where E_{out} and E_{total} represents the total energy delivered to the electrodes and total energy stored in the battery, respectively.

B. Normalised volumetric factor

The second factor to be considered is related to the device volume, more particularly, to the volume of the circuit and output connectors.

Manufacturers usually develop device families (e.g., Infinity™ [118]) consisting on a device group based on a common platform (e.g: same electronics and electrode count), but with different batteries. With such strategy they can offer several devices with different volumes and battery life (in case of primary cell based devices) intended for the same treatment. Sometimes, they leverage the fact that a neurostimulation platform is able to treat different diseases, each requires its own stimulation intensity, sensing, and processing, producing different power consumption. So creating different devices with batteries according to the intended use may tend to reduce overall volume while maintaining longevity. Another factor is the important miniaturisation trend (as depicted in Fig. 13), offering patients the smallest achievable platform in order to maximise take-up. To do so, manufacturers can reuse an already designed platform and transform that to be rechargeable, using a considerable smaller battery. Even though rechargeable capability requires additional circuits to manage charging properly, in general there will be an overall volume reduction. With the consideration mentioned before, the factor F_{Vol} can be estimated by total volume Vol_{total} and battery volume Vol_{batt} as follows:

$$F_{Vol} = Vol_{total} - Vol_{batt}. \tag{13}$$

Since F_{Vol} is independent from battery volume, it is expected to have similar values for all devices out of the same family. Nonetheless, as it was mentioned in Section IV, both circuit and output connector volume depends on electrode number which is tied to device intended use. That renders F_{Vol} dependent on device intended use, which is not suitable for cross-therapy device comparisons. We took the same approach as that implemented in the device volume comparison in Section IV, that is the volumetric factor normalisation (F_{Vol}^{norm}) by the electrode number N_E as follows:

$$F_{Vol}^{norm} = \frac{F_{Vol}}{N_E} = \frac{Vol_{total} - Vol_{batt}}{N_E}. \tag{14}$$

By construction, F_{Vol}^{norm} renders independent from battery selection and device intended use, characteristics we understand are suitable for fairly comparisons between neurostimulators of any kind.

C. Figure of Merit definition

The proposed FoM is defined by F_{Eff} and F_{Vol}^{norm} factors, as follows:

$$FoM = \frac{F_{Eff}}{F_{Vol}^{norm}} = \frac{E_{out}}{E_{total}} \frac{N_E}{Vol_{total} - Vol_{batt}}. \tag{15}$$

Hence, a great FoM stands for either a good energetic efficiency (i.e., a high F_{Eff} factor), an efficient use of device volume (i.e., a low F_{Vol}^{norm} factor), or both simultaneously.

For 14 of the assessed neurostimulation devices that have enough data to compute the energetic and volumetric factors, we computed the FoM along with some research platforms presented in [69], [70] (DyNeuMo), [67] (WAND), and [68] (University of Toronto). Results are presented in Fig. 15. As expected, devices which belongs to the same family (as Infinity 606x DBS devices) present similar FoM. The best results are obtained by NeuroPace RNS, which has the best (i.e., the smallest) volumetric factor. In regard to research platforms, all of them have a FoM greater than that for commercially available devices because of a better volume/electrode relationship, obtained by the use of "non-standard" output connectors. The case of DyNeuMoMk-2 (with a FoM similar to the best figures obtained by commercial devices) is rather different since it is based on the Picostim [119], a platform aimed at being implanted in humans since its conception, having the typical form factor of commercial devices.

TABLE III
MINIMUM DEVICE VOLUME ESTIMATIONS

$$Vol_{total} = Vol_{batt} + Vol_{conn} = \frac{\omega T_{batt}}{V[(1-\kappa)\sigma]} + \epsilon N_E$$

$\kappa = 0.25$; ω AS IN TABLE II

Therapy	Electrode number	[Total volume (cm^3) ‖ Battery volume (%) ‖ Connector volume (%)]				
		Rechargeable: Li-Ion (σ = 98 mAh/cm^3, V = 4.1 V)			Non-rechargeable: Li/CFx-SVO (σ = 333 mAh/cm^3, V = 3.0 V)	
		T$_{batt}$			T$_{batt}$	
		1 day	7 days	30 days	1 year	5 years
VNS - Epilepsy	2	0.18 ‖ <1 ‖ 100	0.18 ‖ 2 ‖ 98	0.19 ‖ 7 ‖ 93	0.24 ‖ 27 ‖ 73	0.50 ‖ 65 ‖ 35
VNS - Stroke	2	0.18 ‖ <1 ‖ 100	0.18 ‖ <1 ‖ 100	0.18 ‖ 1 ‖ 99	0.19 ‖ 6 ‖ 94	0.23 ‖ 24 ‖ 76
VNS - Inflammation	2	0.18 ‖ <1 ‖ 100	0.18 ‖ <1 ‖ 100	0.18 ‖ 2 ‖ 98	0.19 ‖ 8 ‖ 92	0.25 ‖ 29 ‖ 71
SCS	16	1.42 ‖ <1 ‖ 100	1.46 ‖ 3 ‖ 97	1.62 ‖ 13 ‖ 87	2.44 ‖ 42 ‖ 58	6.56 ‖ 79 ‖ 21
SCS HF10	16	1.44 ‖ 2 ‖ 98	1.62 ‖ 13 ‖ 87	2.33 ‖ 39 ‖ 61	5.90 ‖ 76 ‖ 24	23.86 ‖ 94 ‖ 6
DBS - Parkinson	16	1.42 ‖ 1 ‖ 99	1.49 ‖ 5 ‖ 95	1.74 ‖ 19 ‖ 81	3.05 ‖ 54 ‖ 46	9.62 ‖ 85 ‖ 15
PNS	6	0.53 ‖ <1 ‖ 100	0.53 ‖ 1 ‖ 99	0.54 ‖ 3 ‖ 97	0.60 ‖ 12 ‖ 88	0.88 ‖ 40 ‖ 60
HNS	4	0.36 ‖ 1 ‖ 99	0.38 ‖ 8 ‖ 92	0.49 ‖ 28 ‖ 72	1.02 ‖ 66 ‖ 34	3.72 ‖ 91 ‖ 9
SNS	4	0.35 ‖ 1 ‖ 99	0.37 ‖ 4 ‖ 96	0.41 ‖ 14 ‖ 86	0.63 ‖ 44 ‖ 56	1.73 ‖ 80 ‖ 20
RNS	8	0.70 ‖ <1 ‖ 100	0.71 ‖ <1 ‖ 100	0.71 ‖ 1 ‖ 99	0.76 ‖ 7 ‖ 93	0.96 ‖ 27 ‖ 73

$$FoM = \frac{E_{out}}{E_{total}} \frac{N_E}{Vol_{total} - Vol_{batt}}$$
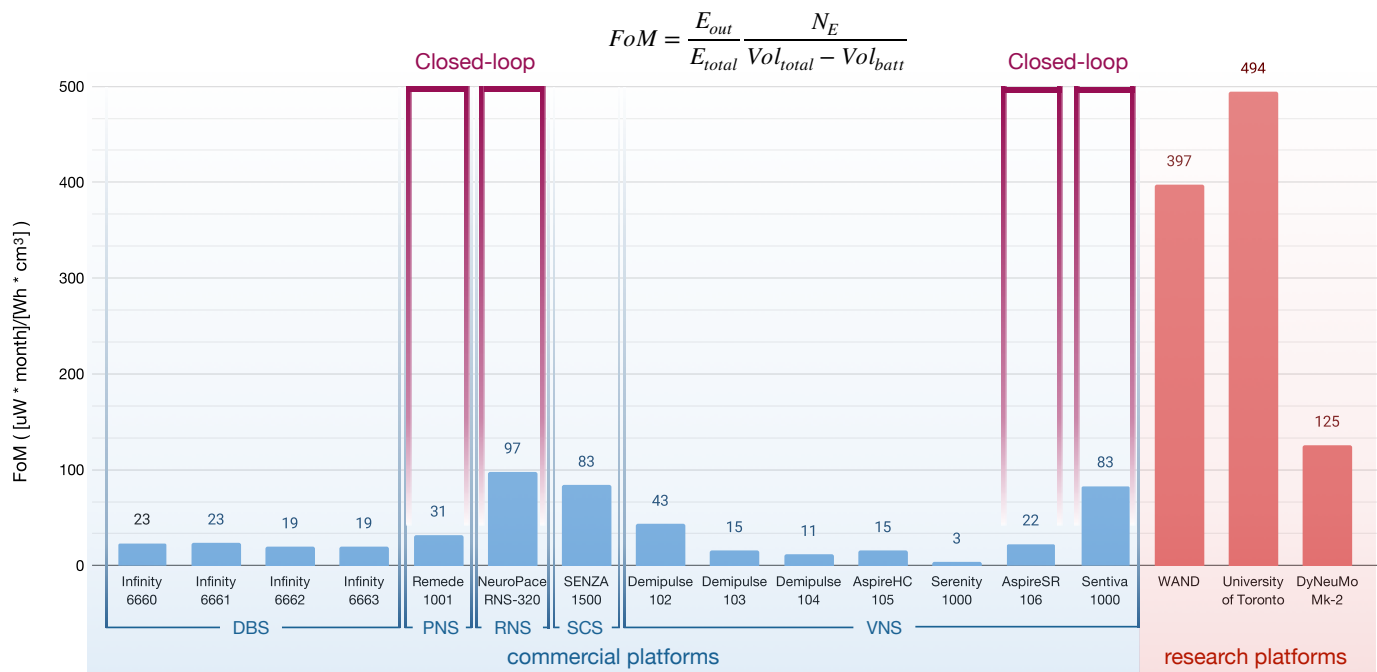
Fig. 15. FoM applied to the assessed devices with enough data to compute the energetic and volumetric factors. Additionally, the FoM was applied to three research platforms. All of them outperform commercially available devices. This is because of a better volume/electrode ratio.

VII. CONCLUSIONS

There has been a surge in translational opportunities within the neurotechnology industry over the past two decades, manifested in an important amount of commercially available implantable neurostimulators aimed at many different neural targets.

From analysing 45 devices, some trends and characteristics in the commercial design of implantable neurostimulators can be demonstrated.

We identified a neurostimulator volume reduction of 0.27 cm^3/electrode per year. The smallest form factor are presented in rechargeable platforms with figures lower than 2 cm^3/electrode.

Notwithstanding their advantage in terms of volume reduction, current rechargeable battery technologies present volumetric energy densities far lower than their non-rechargeable counterparts. This fact limits battery capacity which, along with the broad range of therapy power, increases the patient burden due to frequent recharging processes.

Energetic densities of current battery technologies as well as output connector volume strongly define overall device volume and limit further miniaturisation of the next generation of implantable neurostimulators.

In addition to those limitations, less than 25 % of total energy budget is delivered to the tissue whereas estimations show that more than 50 % of total battery energy is invested in internal activities. From our point of view, this shows that there

is plenty of room for improvement in low power approaches for digital processing as well as therapy power savings by implementing platforms in a closed loop fashion that can save stimulation power by adjusting when and how to stimulate.

A Figure of Merit (FoM) is proposed to compare implantable neurostimulators. Its characteristics render the FoM independent from device intended use, battery technology and capacity, as well as charging capabilities, and electrode number.

The FoM was quantified across 14 of the reviewed devices (those with enough data to do so). Along with these commercial devices three comparable, representative research platforms were benchmarked. A clear gap between these two kind of devices is shown. It is mainly explained by the connector technology used by the research platforms that provides better electrode-volume trade-off.

DATA AVAILABILITY STATEMENT

The data that support the findings of this study has all been derived from the referenced literature. This is summarised in Annex I.

ANNEX I

Herein, we provide a comprehensive reference to all neurostimulators (listed in Table IV) and cardiac pacemakers (listed in Table V) that we reviewed providing key design features/parameters.

REFERENCES

[1] M. Intelligence, "Neuromodulation market," https://www.alliedmarketresearch.com/neurostimulation-devices-market, Accessed on: December 28, 2019.

[2] B.-c. Son, D.-r. Kim, I.-s. Kim, and J. T. Hong, "Phrenic nerve stimulation for diaphragm pacing in a quadriplegic patient," *Journal of Korean Neurosurgical Society*, vol. 54, no. 4, p. 359, 2013.

[3] R. S. Augostini *et al.*, "How to implant a phrenic nerve stimulator for treatment of central sleep apnea?" *Journal of cardiovascular electrophysiology*, vol. 30, no. 5, pp. 792–799, 2019.

[4] M. R. Costanzo *et al.*, "Transvenous neurostimulation for central sleep apnoea: a randomised controlled trial," *The Lancet*, vol. 388, no. 10048, pp. 974–982, 2016.

[5] P. R. Eastwood *et al.*, "Bilateral hypoglossal nerve stimulation for treatment of adult obstructive sleep apnoea," *European Respiratory Journal*, vol. 55, no. 1, 2020.

[6] Inspire, "Inspire upper airway stimulation – p130008/s039," https://www.fda.gov/medical-devices/recently-approved-devices/inspirer-upper-airway-stimulation-p130008s039, 2020.

[7] Inspire, "Inspire upper airway stimulation – report," https://s22.q4cdn.com/384014896/files/doc_presentations/2021/01/08/INSP-Co-Pres-2021-01.pdf, 2021.

[8] A. M. Lozano *et al.*, "Deep brain stimulation: current challenges and future directions," *Nature Reviews Neurology*, vol. 15, no. 3, pp. 148–160, 2019.

[9] R. Fisher *et al.*, "Electrical stimulation of the anterior nucleus of thalamus for treatment of refractory epilepsy," *Epilepsia*, vol. 51, no. 5, pp. 899–908, 2010.

[10] R. Eitan *et al.*, "One year double blind study of high vs low frequency subcallosal cingulate stimulation for depression," *Journal of psychiatric research*, vol. 96, pp. 124–134, 2018.

[11] J. Kuhn *et al.*, "Deep brain stimulation of the nucleus basalis of meynert in alzheimer's dementia," *Molecular psychiatry*, vol. 20, no. 3, pp. 353–360, 2015.

[12] A. M. Lozano and N. Lipsman, "Probing and regulating dysfunctional circuits using deep brain stimulation," *Neuron*, vol. 77, no. 3, pp. 406–424, 2013.

[13] S. Medical, "Setpoint medical reports new data demonstrating its bioelectronic medicine effectively reduces crohn's disease activity," https://setpointmedical.com/category/press-releases/, May 2019.

[14] G. University Hospital, "Vagus nerve stimulation a new approach in the treatment of crohn's disease (vns)," https://clinicaltrials.gov/ct2/show/NCT01569503, 2012.

[15] P. Afra, B. Adamolekun, S. Aydemir, and G. D. R. Watson, "Evolution of the vagus nerve stimulation (vns) therapy system technology for drug-resistant epilepsy," *Frontiers in Medical Technology*, p. 31, 2021.

[16] R. H. McAllister-Williams *et al.*, "The effects of vagus nerve stimulation on the course and outcomes of patients with bipolar disorder in a treatment-resistant depressive episode: a 5-year prospective registry," *International journal of bipolar disorders*, vol. 8, no. 1, pp. 1–11, 2020.

[17] B. Dell'Osso, L. Oldani, B. Grancini, A. Dario *et al.*, "Ten-year outcome of vagus nerve stimulation-implanted patients with treatment-resistant depression: two italian cases," *Neuropsychiatric Disease and Treatment*, vol. 14, p. 915, 2018.

[18] M. S. George *et al.*, "A pilot study of vagus nerve stimulation (vns) for treatment-resistant anxiety disorders," *Brain stimulation*, vol. 1, no. 2, pp. 112–121, 2008.

[19] R. H. Howland, "Vagus nerve stimulation," *Current behavioral neuroscience reports*, vol. 1, no. 2, pp. 64–73, 2014.

[20] M. Jarrett *et al.*, "Systematic review of sacral nerve stimulation for faecal incontinence and constipation," *Journal of British Surgery*, vol. 91, no. 12, pp. 1559–1569, 2004.

[21] E. A. Tanagho and R. A. Schmidt, "Bladder pacemaker: scientific basis and clinical future," *Urology*, vol. 20, no. 6, pp. 614–619, 1982.

[22] S. S. Steele, "Sacral nerve stimulation: 50 years in the making," *Canadian Urological Association Journal*, vol. 6, no. 4, p. 231, 2012.

[23] K. M. Peters, J. M. Carey, and D. B. Konstandt, "Sacral neuromodulation for the treatment of refractory interstitial cystitis: outcomes based on technique," *International Urogynecology Journal*, vol. 14, no. 4, pp. 223–228, 2003.

[24] K.-D. Sievert *et al.*, "Early sacral neuromodulation prevents urinary incontinence after complete spinal cord injury," *Annals of neurology*, vol. 67, no. 1, pp. 74–84, 2010.

[25] B. Govaert, Y. Maeda, J. Alberga, S. Buntzen *et al.*, "Medium-term outcome of sacral nerve modulation for constipation," *Diseases of the colon & rectum*, vol. 55, no. 1, pp. 26–31, 2012.

[26] A. P. Cameron *et al.*, "National trends in the usage and success of sacral nerve test stimulation," *The Journal of urology*, vol. 185, no. 3, pp. 970–975, 2011.

[27] P. L. Gildenberg, "History of electrical neuromodulation for chronic pain," pp. S7–S13, 2006.

[28] J. Caylor *et al.*, "Spinal cord stimulation in chronic pain: evidence and theory for mechanisms of action," *Bioelectronic medicine*, vol. 5, no. 1, pp. 1–41, 2019.

[29] N. P. Release, "Nevro receives fda approval for senza spinal cord stimulation system delivering hf10 therapy," https://www.nevro.com/English/us/about/newsroom/default.aspx, May 2015.

[30] J. M. Hagedorn, A. Layno-Moses, D. T. Sanders, D. J. Pak *et al.*, "Overview of hf10 spinal cord stimulation for the treatment of chronic pain and an introduction to the senza omnia system," *Pain Management*, vol. 10, no. 6, pp. 367–376, 2020.

[31] P. P. Management, "FDA approves new 'burst' device for spinal cord stimulation," https://www.practicalpainmanagement.com/, Oct. 2015.

[32] T. Deer *et al.*, "Success using neuromodulation with burst (sunburst) study: results from a prospective, randomized controlled trial using a novel burst waveform," *Neuromodulation: Technology at the Neural Interface*, vol. 21, no. 1, pp. 56–66, 2018.

[33] FDA, "Summary of safety and effectiveness data (ssed) for senza spinal cord stimulation (scs) system," 2015.

[34] J. Prager, "Estimates of annual spinal cord stimulator implant rises in the united states," *Neuromodulation: Technology at the Neural Interface*, vol. 1, no. 13, pp. 68–69, 2010.

[35] A. D. Sdrulla, Y. Guan, and S. N. Raja, "Spinal cord stimulation: clinical efficacy and potential mechanisms," *Pain Practice*, vol. 18, no. 8, pp. 1048–1067, 2018.

TABLE IV
NEUROMODULATION DEVICES

Device	Neural target	Volume (cm³)	Released year	Electrode number	Chemistry	Battery type	Capacity (mAh)	Batt. volt (V)	Batt. vol (cm³)	Current (mA)	Frequency (Hz)	Pulse width (μs)	Consumption Amp. (mA)	Consumption Freq. (Hz)	Consumption Pulse width (μs)	Consumption Duty cycle	Consumption Balance	Z (Ω)	Batt. life (months)
SetPoint [120]	VNS	2	2012	2	Li-Ion	Rechargeable	2.8	3.6	—	—	—	—	—	—	—	—	—	3000	114
Demi103 [121], [122], [15]	VNS	9.9	2007	2	Li/CFx	Primary	1000	3.3	2.99	0.0-3.5	1-30	130-1000	0.50	30	130	0.50	1	3000	114
Demi104 [121], [15]	VNS	12.1	2007	2	Li/CFx	Primary	1000	3.3	2.99	0.0-3.5	1-30	130-1000	0.50	30	130	0.50	1	3000	58.8[10]
Demi102/R [121], [15]	VNS	18.7	2003	2	Li/CFx	Primary	1700	3.3	4.92	0.0-3.5	1-30	130-1000	1.5	30	130	0.5	1	3000	103.2
AspireHC105 [121], [15]	VNS	18.7	2010	2	Li/CFx	Primary	1700	3.3	4.92	0.0-3.5	1-30	130-1000	0.50	30	500	0.50	1	3000	99.6[9]
AspireSR106 [121], [15]	VNS	18.7	2014	2	Li/CFx	Primary	1700	3.3	4.92	0.0-3.5	1-30	130-1000	1.5	30	250	0.50	1	3000	60
Sentiva1000 [123], [121], [15]	VNS	9.9	2017	2	Li/CFx	Primary	1000	3.3	2.99	0.0-3.5	1-30	130-1000	1.50	20	750	0.51	0	3000	60
Serenity1000 [124], [125], [126]	VNS	34.2	2013	2	Li/CFx	Primary	2500	3.3	7.9	0.0-3.5	1-30	10-1000	1.50	50	500	0.03	0	3000	60
Brio 6789 [127], [128]	DBS	17.7	2013	16	—	Rechargeable	—	—	—	0.0-12.75	2-240	50-500	—	—	—	—	—	—	—
VercisePC [129], [130], [131], [132]	DBS	33	2015	8	—	Primary	7500	—	—	0.1-20	2-255	20-450	3	185	60	—	1	1500	0.73
VerciseGevia [129], [130], [133], [134]	DBS	19.8	2017	16	—	Rechargeable	—	—	—	0.1-20	2-255	20-450	3	130	60	—	1	1000	1.02
VerciseGenusP16 [135], [136]	DBS	34.9	2020	16	—	Primary	—	—	—	0.1-20	2-255	20-450	—	—	—	—	—	—	—
VerciseGenusR16 [135], [136]	DBS	20.1	2020	16	—	Rechargeable	—	—	—	0.1-20	2-255	20-450	—	—	—	—	—	—	—
ActivaSC [137], [138], [139]	DBS	27	2011	4	Li/CFx-SVO	Primary	4470	3.2	—	0.0-10.5	2-250	60-450	3	180	60	0.67	0	1000	54
Infinity6660 [118], [140], [141], [142], [143]	DBS	30.4	2015	16	Li/CFx-SVO	Primary	5300	3.25[7]	12.22	0.0-12.75	2-240	20-500	1	120	250	1	1	500	60[4]
Infinity6661 [118], [140], [141], [142], [143]	DBS	30.4	2015	16	Li/CFx-SVO	Primary	5300	3.25[7]	12.22	0.0-12.75	2-240	20-500	1	120	250	—	—	500	60[4]
Infinity6662 [118], [140], [141], [142], [143]	DBS	38.6	2015	16	Li/CFx-SVO	Primary	7500	3.25[8]	17.25	0.0-12.75	2-240	20-500	1	120	250	—	—	500	84[4]
Infinity6663 [118], [140], [141], [142], [143]	DBS	38.6	2015	16	Li/CFx-SVO	Primary	7500	3.25[8]	17.25	0.0-12.75	2-240	20-500	1	120	250	0.67	1	500	84[4]
ActivaPC [137], [138], [144], [145], [146], [147]	DBS	39	2009	8	Li/CFx-SVO	Primary	6300	3.2	—	0.0-10.5[1]	2-250[1]	60-450	3	180	60	0.67	0	1000	84
ActivaRC [137], [148], [138], [146]	DBS	22	2009	8	Li-Ion	Rechargeable	500	3.7	—	0.0-10.5[1]	2-250[1]	60-450	3	185	60	—	0	1200	0.86
PerceptPC [149], [150], [151], [152], [138], [63]	DBS	33	2019	16	Li/CFx-SVO	Primary	—	—	—	—	2-250	20-450	—	—	—	—	—	—	—
LibraXP [128]	DBS	49	2013	8	—	Primary	—	—	—	0.0-12.75	2-200	52-507	—	—	—	—	—	—	—
NeuroPaceRNS-320 [102], [153]	RNS	11	2013	8	Li/CFx-SVO	Primary	1114	3.2	4.4[2]	0.0-12	1-333	40-1000	6	200	160	6.6e-4[6]	1	1000	100.8
InterstimMicro [154]	SNS	2.8	2020	4	—	Rechargeable	—	—	—	—	—	—	—	—	—	—	—	—	—
InterStimX [155]	SNS	12.5	2022	4	—	Primary	1200	—	—	—	—	—	—	—	—	—	—	—	—
Interstim2 [154], [156]	SNS	14	2006	4	—	Primary	1300	—	—	—	—	—	—	—	—	—	—	—	—
Axonics [156], [157], [158], [159]	SNS	5.5	2016	4	Li-Ion	Rechargeable	50	—	—	—	40-1200	60-1000	—	—	—	—	—	—	—
Intellis [160], [161], [162], [163]	SCS	13.9	2017	16	—	Rechargeable	—	—	—	0.0-25.5	2-1200	50-500	3	40	200	1	0	500	4.03
EonMini [164], [165]	SCS	18	2008	16	—	Rechargeable	—	—	—	0.0-25.5	2-1200	60-1000	3	40	200	1	1	500	1.80
RestoreULTRA [164], [166], [163]	SCS	22	2013	16	—	Rechargeable	—	—	—	0.0-25.5	—	—	3	—	—	—	—	—	—
RestoreSensor37714 [167], [163]	SCS	22	2011	16	—	Rechargeable	—	—	—	—	—	—	—	—	—	—	—	—	—
PrimeAdvanced37702 [163], [168]	SCS	39	2006	16	—	Primary	—	—	—	—	—	—	—	—	—	—	—	—	—
RestoreAdvanced97713 [163], [169]	SCS	39	2013	16	—	Rechargeable	—	—	—	—	—	—	—	—	—	—	—	—	—
Itrel4 [163], [170]	SCS	28	2012	4	—	Primary	4500	—	—	—	—	—	—	—	—	—	—	—	—
PrecisionSpectra [164], [171]	SCS	22	2013	32	Li-Ion	Rechargeable	180	3.6	—	0.0-25.5	2-1200	20-1000	3	40	200	1	0	500[3]	2.03
PrecisionMontage [171], [172]	SCS	18	2016	16	—	Rechargeable	—	—	—	—	—	—	—	—	—	—	—	—	—
PrecisionNovi [171], [173]	SCS	33	2015	16	—	Primary	—	—	—	—	—	—	—	—	—	—	—	—	—
PrecisionPlus [171], [174]	SCS	22	2012	16	—	Rechargeable	—	—	—	—	—	—	—	—	—	—	—	—	—
Prodigy3772 [175], [176]	SCS	17.7	2015	16	—	Rechargeable	—	—	—	—	—	—	—	—	—	—	—	—	—
Proclaim3660 [177], [178]	SCS	30	2016	16	Li/CFx-SVO	Primary	5300	3.25	—	0.0-12.75	2-1200	20-1000	5	50	225	0.50	0	500	54
Proclaim3662 [177], [178]	SCS	39	2016	—	—	Primary	7500	—	—	—	—	—	—	—	—	—	—	—	—
SENZA1500 [179], [180], [181]	SCS	41	2010	16	Li-Ion	Rechargeable	440	3.6	5.97	0.0-15	2-10000	20-1000	3.8[5]	10000	30	0.50	1	500[3]	0.13
Evoke SCS [182]	SCS	33	2019	24	Li-Ion	Rechargeable	200	—	—	0.0-5	20-40	60-210	—	—	—	—	—	—	—
Inspire II [183]	HNS	23	2013	4	—	Primary	—	—	—	—	—	—	5	20	150	0.14	0	1000	127.20
Remede1001 [184], [185]	PNS	39	2010	7	Li/CFx	Primary	2200	2.95	15.6[2]	—	20-40	60-210	5	20	150	0.14	0	1000	41

1 Voltage mode.
2 Estimating that battery volume accounts for 40% of overall device volume.
3 Estimated based on typical impedance for the neural target.
4 Energy factor of 60. Software version 1.1.2.1. Unilateral stimulation.
5 Selected to estimate consumption based on maximum (mean) amplitude in order to obtain optimal analgesic response as in [112].
6 Considering 100 ms burst duration, and 570 burst per day.
7 Considering Greatbatch 2477 battery.
8 Considering Greatbatch 2880 battery.
9 AutoStim feature disabled.
10 dc-dc converter code 2.

TABLE V
CARDIAC PACEMAKERS

Device	Manufacturer	Volume (cm^3)	Released year	Electrode number	Chemistry	Battery type	Capacity (mAh)	Batt. volt (V)
Advisa SR [186]	Medtronic	11.9	2018	2	Li/CFx-SVO	Primary	1150	3.2
Azure XT [187], [188]	Medtronic	12.3	2017	4	Li/CFx-SVO	Primary	1200	3.25
Micra AV [106], [189]	Medtronic	1	2020	2	Li/CFx-SVO	Primary	120	3.2
Accolade SR [190]	Boston Scientific	11.7	2016	2	Li/CFx	Primary	1000	—
Accolade DR [190]	Boston Scientific	12.2	2016	4	Li/CFx	Primary	1000	—
Accolade DR [190]	Boston Scientific	14.2	2016	4	Li/CFx	Primary	1600	—
Essentio SR [190]	Boston Scientific	11.7	2016	2	Li/CFx	Primary	1000	—
Essentio DR [190]	Boston Scientific	12.2	2016	4	Li/CFx	Primary	1000	—
Essentio DR [190]	Boston Scientific	14.2	2016	4	Li/CFx	Primary	1600	—
Ingenio SR [190]	Boston Scientific	11.5	2012	2	Li/CFx-SVO	Primary	1050	—
Ingenio DR [190]	Boston Scientific	12	2012	4	Li/CFx-SVO	Primary	1050	—
Ingenio DR EL [190]	Boston Scientific	14	2012	4	LiMO	Primary	1470	—
Vitalio SR [190], [191]	Boston Scientific	12	2013	2	Li/CFx-SVO	Primary	1050	—
Vitalio DR [190], [191]	Boston Scientific	12	2013	4	Li/CFx-SVO	Primary	1050	—
Vitalio DR EL [190], [191]	Boston Scientific	14	2013	4	LiMO	Primary	1470	—
ENO DR [192]	MicroPort	8.0	2019	4	Li-I2	Primary	810	2.8
ENO SR [192]	MicroPort	7.5	2019	2	Li-I2	Primary	810	2.8
TEO DR [193]	MicroPort	8.0	2019	4	Li-I2	Primary	810	2.8
TEO SR [193]	MicroPort	7.5	2019	2	Li-I2	Primary	810	2.8
OTO DR [194]	MicroPort	8.0	2019	4	Li-I2	Primary	810	2.8
OTO SR [194]	MicroPort	7.5	2019	2	Li-I2	Primary	810	2.8

[36] NeurologyLive, "FDA approves Saluda's Evoke spinal cord stimulation system for chronic intractable pain," https://www.neurologylive.com/, Mar. 2022.

[37] N. Mekhail et al., "Long-term safety and efficacy of closed-loop spinal cord stimulation to treat chronic back and leg pain (evoke): a double-blind, randomised, controlled trial," The Lancet Neurology, vol. 19, no. 2, pp. 123–134, 2020.

[38] K. Famm, B. Litt, K. J. Tracey, E. S. Boyden et al., "A jump-start for electroceuticals," Nature, vol. 496, no. 7444, pp. 159–161, 2013.

[39] A. Majid, Electroceuticals: Advances in electrostimulation therapies. Springer, Jan. 2017.

[40] M. Donegà et al., "Human-relevant near-organ neuromodulation of the immune system via the splenic nerve," Proceedings of the National Academy of Sciences, vol. 118, no. 20, 2021.

[41] C. Sarica et al., "Implantable pulse generators for deep brain stimulation: Challenges, complications, and strategies for practicality and longevity," Frontiers in Human Neuroscience, vol. 15, 2021. https://www.frontiersin.org/article/10.3389/fnhum.2021.708481

[42] D. Guiraud et al., "Vagus nerve stimulation: state of the art of stimulation and recording strategies to address autonomic function neuromodulation," Journal of Neural Engineering, vol. 13, no. 4, p. 041002, Jun. 2016. https://doi.org/10.1088/1741-2560/13/4/041002

[43] M. Vissani, I. U. Isaias, and A. Mazzoni, "Deep brain stimulation: a review of the open neural engineering challenges," Journal of Neural Engineering, vol. 17, no. 5, p. 051002, Oct. 2020. https://doi.org/10.1088/1741-2552/abb581

[44] G. L. Barbruni, P. M. Ros, D. Demarchi, S. Carrara et al., "Miniaturised wireless power transfer systems for neurostimulation: A review," IEEE Transactions on Biomedical Circuits and Systems, vol. 14, no. 6, pp. 1160–1178, 2020.

[45] R. Das, F. Moradi, and H. Heidari, "Biointegrated and wirelessly powered implantable brain devices: A review," IEEE Transactions on Biomedical Circuits and Systems, vol. 14, no. 2, pp. 343–358, 2020.

[46] S. B. Goncalves, J. F. Ribeiro, A. F. Silva, R. M. Costa et al., "Design and manufacturing challenges of optogenetic neural interfaces: a review," Journal of Neural Engineering, vol. 14, no. 4, p. 041001, May 2017. https://doi.org/10.1088/1741-2552/aa7004

[47] J. Koch, M. Schuettler, C. Pasluosta, and T. Stieglitz, "Electrical connectors for neural implants: Design, state of the art and future challenges of an underestimated component," Journal of Neural Engineering, vol. 16, no. 6, Oct. 2019.

[48] N. K. Ann, G. Elliot, X. Y. Ping, and T. N. V., "Implantable neurotechnologies: a review of integrated circuit neural amplifiers," Medical & Biological Engineering & Computing, vol. 54, no. 1, Jan. 2016. https://doi.org/10.1007/s11517-015-1431-3

[49] M. Parastarfeizabadi and A. Z. Kouzani, "Advances in closed-loop deep brain stimulation devices," Journal of neuroengineering and rehabilitation, vol. 14, no. 1, p. 79, Aug. 2017.

[50] P. Khanna et al., "Enabling closed-loop neurostimulation research with downloadable firmware upgrades," in IEEE Biomedical Circuits and Systems Conference: Engineering for Healthy Minds and Able Bodies, BioCAS 2015 - Proceedings. Institute of Electrical and Electronics Engineers Inc., Dec. 2015.

[51] H. Kassiri, S. Tonekaboni, M. T. Salam, N. Soltani et al., "Closed-loop neurostimulators: A survey and a seizure-predicting design example for intractable epilepsy treatment," IEEE transactions on biomedical circuits and systems, vol. 11, no. 5, pp. 1026–1040, 2017.

[52] B. Zhu, U. Shin, and M. Shoaran, "Closed-loop neural prostheses with on-chip intelligence: A review and a low-latency machine learning model for brain state detection," IEEE Transactions on Biomedical Circuits and Systems, 2021.

[53] R. Vallejo, A. W. Krishnan Chakravarthy, K. Trutnau, and D. Dinsmoor, "A new direction for closed-loop spinal cord stimulation: Combining contemporary therapy paradigms with evoked compound action potential sensing," Journal of Pain Research, vol. 14, p. 3909, 2021.

[54] C. M. Wray and E. R. Thaler, "Hypoglossal nerve stimulation for obstructive sleep apnea: A review of the literature," World journal of otorhinolaryngology-head and neck surgery, vol. 2, no. 04, pp. 230–233, 2016.

[55] N. Ding and X. Zhang, "Transvenous phrenic nerve stimulation, a novel therapeutic approach for central sleep apnea," Journal of Thoracic Disease, vol. 10, no. 3, p. 2005, 2018.

[56] A. Zhou, B. C. Johnson, and R. Muller, "Toward true closed-loop neuromodulation: artifact-free recording during stimulation," Current Opinion in Neurobiology, vol. 50, pp. 119–127, Jun. 2018.

[57] M. Arlotti, M. Colombo, A. Bonfanti, T. Mandat et al., "A new implantable closed-loop clinical neural interface: first application in parkinson's disease," Frontiers in Neuroscience, vol. 15, 2021.

[58] Newronika, "NCT04681534: Safety and efficacy of adaptive deep brain stimulation," https://clinicaltrials.gov/ct2/show/NCT04681534, Jan. 2021.

[59] J. L. Collinger et al., "High-performance neuroprosthetic control by an individual with tetraplegia," The Lancet, vol. 381, no. 9866, pp. 557–564, 2013.

[60] A. B. Rapeaux and T. G. Constandinou, "Implantable brain machine interfaces: first-in-human studies, technology challenges and trends," Current opinion in biotechnology, vol. 72, pp. 102–111, 2021.

[61] D. Seo, J. M. Carmena, J. M. Rabaey, E. Alon et al., "Neural dust: An ultrasonic, low power solution for chronic brain-machine interfaces," arXiv preprint arXiv:1307.2196, 2013.

[62] R. Melzack and P. D. Wall, "Pain mechanisms: A new theory: A gate control system modulates sensory input from the skin before it evokes pain perception and response." *Science*, vol. 150, no. 3699, pp. 971–979, 1965.

[63] S. C. *et al.*, "Implantable Pulse Generators for Deep Brain Stimulation: Challenges, Complications, and Strategies for Practicality and Longevity," *Frontiers in Human Neuroscience*, Aug. 2021.

[64] S. Stanslaski, J. Herron, T. Chouinard, D. Bourget *et al.*, "A chronically implantable neural coprocessor for investigating the treatment of neurological disorders," *IEEE transactions on biomedical circuits and systems*, vol. 12, no. 6, pp. 1230–1245, 2018.

[65] M. Gaidica and B. Dantzer, "An implantable neurophysiology platform: Broadening research capabilities in free-living and non-traditional animals." *Frontiers in neural circuits*, vol. 16, pp. 940 989–940 989, 2022.

[66] S. Reich, M. Sporer, M. Haas, J. Becker *et al.*, "A high-voltage compliance, 32-channel digitally interfaced neuromodulation system on chip," *IEEE Journal of Solid-State Circuits*, vol. 56, no. 8, pp. 2476–2487, 2021.

[67] A. Zhou *et al.*, "A wireless and artefact-free 128-channel neuromodulation device for closed-loop stimulation and recording in non-human primates," *Nature biomedical engineering*, vol. 3, no. 1, pp. 15–26, 2019.

[68] A. Bagheri *et al.*, "Massively-parallel neuromonitoring and neurostimulation rodent headset with nanotextured flexible microelectrodes," *IEEE Transactions on biomedical circuits and systems*, vol. 7, no. 5, pp. 601–609, 2013.

[69] R. Toth *et al.*, "Dyneumo mk-2: an investigational circadian-locked neuromodulator with responsive stimulation for applied chronobiology," in *2020 IEEE International Conference on Systems, Man, and Cybernetics (SMC)*. IEEE, 2020, pp. 3433–3440.

[70] M. Zamora, R. Toth, F. Morgante, J. Ottaway *et al.*, "Dyneumo mk-1: Design and pilot validation of an investigational motion-adaptive neurostimulator with integrated chronotherapy," *Experimental Neurology*, vol. 351, p. 113977, 2022.

[71] K. Fakhar, E. Hastings, C. Butson, K. Foote *et al.*, "Management of deep brain stimulator battery failure: battery estimators, charge density, and importance of clinical symptoms," *PLoS One*, Mar. 2013.

[72] M. Niemann, G.-H. Schneider, A. Kühn, P. Vajkoczy *et al.*, "Longevity of implantable pulse generators in bilateral deep brain stimulation for movement disorders," *Neuromodulation: Technology at the Neural Interface*, vol. 21, no. 6, pp. 597–603, 2018.

[73] D. R. Merrill, M. Bikson, and J. G. Jefferys, "Electrical stimulation of excitable tissue: design of efficacious and safe protocols," *Journal of neuroscience methods*, vol. 141, no. 2, pp. 171–198, 2005.

[74] F. Eshaghi, T. Moeinfard, E. Najafiaghdam, and H. Kassiri, "A neurostimulator IC with impedance-aware dynamic-precision one-shot charge balancing," *IEEE Solid-State Circuits Letters*, vol. 4, pp. 202–205, 2021.

[75] R. Guan, P. G. Zufiria, V. Giagka, and W. A. Serdijn, "Circuit design considerations for power-efficient and safe implantable electrical neurostimulators," in *2020 IEEE 11th Latin American Symposium on Circuits & Systems (LASCAS)*. IEEE, 2020, pp. 1–4.

[76] X. Liu, A. Demosthenous, and N. Donaldson, "An integrated implantable stimulator that is fail-safe without off-chip blocking-capacitors," *IEEE Transactions on Biomedical Circuits and Systems*, vol. 2, no. 3, pp. 231–244, 2008.

[77] H. Kassiri, M. T. Salam, M. R. Pazhouhandeh, N. Soltani *et al.*, "Rail-to-rail-input dual-radio 64-channel closed-loop neurostimulator," *IEEE Journal of Solid-State Circuits*, vol. 52, no. 11, pp. 2793–2810, 2017.

[78] F. Kolbl, Y. Bornat, J. Castelli, L. Regnacq *et al.*, "Ic-based neuro-stimulation environment for arbitrary waveform generation," *Electronics*, vol. 10, no. 15, p. 1867, 2021.

[79] E. Greenwald, C. Maier, Q. Wang, R. Beaulieu *et al.*, "A cmos current steering neurostimulation array with integrated dac calibration and charge balancing," *IEEE transactions on biomedical circuits and systems*, vol. 11, no. 2, pp. 324–335, 2017.

[80] R. Shulyzki, K. Abdelhalim, A. Bagheri, M. T. Salam *et al.*, "320-channel active probe for high-resolution neuromonitoring and responsive neurostimulation," *IEEE transactions on biomedical circuits and systems*, vol. 9, no. 1, pp. 34–49, 2014.

[81] Y. Wu, D. Jiang, and A. Demosthenous, "A multi-channel stimulator with high-resolution time-to-current conversion for vagal-cardiac neuromodulation," *IEEE Transactions on Biomedical Circuits and Systems*, vol. 15, no. 6, pp. 1186–1195, 2021.

[82] X. Liu, A. Demosthenous, and N. Donaldson, "Neural interfaces for implanted stimulators," in *Springer Handbook of Medical Technology*. Springer, 2011, pp. 749–766.

[83] BSI, "BS EN 45502-1:2015 Implants for surgery - Active implantable medical devices - General requirements for safety, marking and for information to be provided by the manufacturer." British Standards Publication, Standard, Jun. 2015.

[84] ISO, "ISO 14708-3:2017 Implants for surgery — Active implantable medical devices — Part 3: Implantable neurostimulators," International Organization for Standardization, Standard, Apr. 2017.

[85] ISO, "ISO 14708-1:2014 Implants for surgery — Active implantable medical devices — Part 1: General requirements for safety, marking and for information to be provided by the manufacturer." International Organization for Standardization, Standard, Aug. 2014.

[86] W. Biederman *et al.*, "A 4.78 mm2 Fully-Integrated Neuromodulation SoC Combining 64 Acquisition Channels with Digital Compression and Simultaneous Dual Stimulation," *IEEE Journal of Solid-State Circuits*, vol. 50, no. 4, pp. 1038–1047, Apr. 2015.

[87] ISO, "ISO 14971 Medical devices - Application of risk management to medical devices." International Organization for Standardization, Standard, Dec. 2019.

[88] IEC, "IEC 62304 Medical device software - Software life cycle processes." International Organization for Standardization, Standard, Jun. 2015.

[89] A. M. Koss, R. L. Alterman, M. Tagliati, and J. L. Shils, "Calculating total electrical energy delivered by deep brain stimulation systems," *Annals of neurology*, vol. 58, no. 1, p. 168, 2005.

[90] E. Moro *et al.*, "Bilateral globus pallidus stimulation for huntington's disease," *Annals of Neurology: Official Journal of the American Neurological Association and the Child Neurology Society*, vol. 56, no. 2, pp. 290–294, 2004.

[91] D. Hui, A. Murgai, G. Gilmore, S. Mohideen *et al.*, "Assessing the effect of current steering on the total electrical energy delivered and ambulation in parkinson's disease," *Scientific Reports*, vol. 10, May 2020.

[92] S. D. Israeli-Korn *et al.*, "Decreasing battery life in subthalamic deep brain stimulation for parkinson's disease with repeated replacements: Just a matter of energy delivered?" *Brain Stimulation*, vol. 12, no. 4, pp. 845–850, 2019. https://www.sciencedirect.com/science/article/pii/S1935861X19300610

[93] A.-K. Helmers *et al.*, "Comparison of the battery life of nonrechargeable generators for deep brain stimulation," *Neuromodulation: Technology at the Neural Interface*, vol. 21, no. 6, pp. 593–596, 2018.

[94] M. Bin-Mahfoodh, C. Hamani, E. Sime, and A. M. Lozano, "Longevity of batteries in internal pulse generators used for deep brain stimulation," *Stereotactic and functional neurosurgery*, vol. 80, no. 1-4, pp. 56–60, 2003.

[95] H. Chen, M. Liu, W. Hao, Y. Chen *et al.*, "Low-power circuits for the bidirectional wireless monitoring system of the orthopedic implants," *IEEE transactions on biomedical circuits and systems*, vol. 3, no. 6, pp. 437–443, 2009.

[96] L. George, G. D. Gargiulo, T. Lehmann, and T. J. Hamilton, "A 0.04 mm^2 buck-boost dc-dc converter for biomedical implants using adaptive gain and discrete frequency scaling control," *IEEE Transactions on Biomedical Circuits and Systems*, vol. 10, no. 3, pp. 668–678, 2015.

[97] H. S. Gougheri, P. Graybill, and M. Kiani, "A dual-output reconfigurable shared-inductor boost-converter/current-mode inductive power management asic with 750% extended output-power range, adaptive switching control, and voltage-power regulation," *IEEE transactions on biomedical circuits and systems*, vol. 13, no. 5, pp. 1075–1086, 2019.

[98] W.-Y. Hsu and A. Schmid, "Compact, energy-efficient high-frequency switched capacitor neural stimulator with active charge balancing," *IEEE transactions on biomedical circuits and systems*, vol. 11, no. 4, pp. 878–888, 2017.

[99] F. Mounaim and M. Sawan, "Toward a fully integrated neurostimulator with inductive power recovery front-end," *IEEE transactions on biomedical circuits and systems*, vol. 6, no. 4, pp. 309–318, 2012.

[100] A. Urso, V. Giagka, M. van Dongen, and W. A. Serdijn, "An ultra high-frequency 8-channel neurostimulator circuit with 68% peak power efficiency," *IEEE Transactions on Biomedical Circuits and Systems*, vol. 13, no. 5, pp. 882–892, 2019.

[101] I. Williams and T. G. Constandinou, "An energy-efficient, dynamic voltage scaling neural stimulator for a proprioceptive prosthesis," *IEEE Transactions on Biomedical Circuits and Systems*, vol. 7, no. 2, pp. 129–139, 2013.

[102] NeuroPace, *NeuroPace RNS System - Physician Manual*, 2021.

[103] S.-Y. Yang, V. Sencadas, S. S. You, N. Z.-X. Jia *et al.*, "Powering implantable and ingestible electronics," *Advanced functional materials*, vol. 31, no. 44, p. 2009289, 2021.

[104] D. Linden and T. B. Reddy, *Handbook of batteries*. McGraw-Hill, 2002.

[105] D. C. Bock, A. C. Marschilok, K. J. Takeuchi, and E. S. Takeuchi, "Batteries used to power implantable biomedical devices," *Electrochimica acta*, vol. 84, pp. 155–164, 2012.

[106] Medtronic, *Micra MC1VR01 - Clinician Manual*, 2018.

[107] A. Khalifa, S. Lee, A. C. Molnar, and S. Cash, "Injectable wireless microdevices: challenges and opportunities," *Bioelectronic Medicine*, vol. 7, no. 1, pp. 1–8, 2021.

[108] ISO, "27186:2020 Active implantable medical devices -Four-pole connector system for implantable cardiac rhythm management devices - Dimensional and test requirements," International Organization for Standardization, Tech. Rep., 2020.

[109] B. Fisher, J. A. DesMarteau, E. H. Koontz, S. J. Wilks *et al.*, "Responsive vagus nerve stimulation for drug resistant epilepsy: A review of new features and practical guidance for advanced practice providers," *Frontiers in Neurology*, vol. 11, 2021. https://www.frontiersin.org/article/10.3389/fneur.2020.610379

[110] N. D. Engineer, T. J. Kimberley, C. N. Prudente, J. Dawson *et al.*, "Targeted vagus nerve stimulation for rehabilitation after stroke," *Frontiers in Neuroscience*, vol. 13, 2019. https://www.frontiersin.org/article/10.3389/fnins.2019.00280

[111] A. S. Caravaca *et al.*, "An effective method for acute vagus nerve stimulation in experimental inflammation," *Frontiers in Neuroscience*, vol. 13, 2019. https://www.frontiersin.org/article/10.3389/fnins.2019.00877

[112] L. Kapural *et al.*, "Novel 10-kHz High-frequency Therapy (HF10 Therapy) Is Superior to Traditional Low-frequency Spinal Cord Stimulation for the Treatment of Chronic Back and Leg Pain: The SENZA-RCT Randomized Controlled Trial," *Anesthesiology*, vol. 123, no. 4, pp. 851–860, Oct. 2015. https://doi.org/10.1097/ALN.0000000000000774

[113] S. Bratsos, D. Karponis, and S. N. Saleh, "Efficacy and safety of deep brain stimulation in the treatment of parkinson's disease: a systematic review and meta-analysis of randomized controlled trials," *Cureus*, vol. 10, no. 10, 2018.

[114] M. Fudim *et al.*, "Phrenic nerve stimulation for the treatment of central sleep apnea: A pooled cohort analysis," *Journal of Clinical Sleep Medicine*, vol. 15, no. 12, pp. 1747–1755, 2019. https://jcsm.aasm.org/doi/abs/10.5664/jcsm.8076

[115] M. Pengo and j. steier, "Emerging technology: Electrical stimulation in obstructive sleep apnoea," *Journal of Thoracic Disease*, Apr. 2014.

[116] S. Siegel *et al.*, "Five-year followup results of a prospective, multicenter study of patients with overactive bladder treated with sacral neuromodulation," *The Journal of Urology*, vol. 199, no. 1, pp. 229–236, 2018. https://www.sciencedirect.com/science/article/pii/S0022534717770991

[117] D. R. Nair *et al.*, "Nine-year prospective efficacy and safety of brain-responsive neurostimulation for focal epilepsy," *Neurology*, vol. 95, no. 9, pp. e1244–e1256, 2020. https://n.neurology.org/content/95/9/e1244

[118] St. Jude Medical, *St. Jude Medical Infinity Implantable Pulse Generator Models 6660, 6661, 6662, 6663*, 2016.

[119] Bioinduction, "Picostim Cranial DBS," https://bioinduction.com/the-solution/, Accessed on: July 26, 2022.

[120] SetPoint Medical, "Safety and efficacy of vagus nerve stimulator in patients with rheumatoid arthritis (RA)," https://clinicaltrials.gov/ct2/show/NCT03437473, Dec. 2018.

[121] Livanova, *VNS Therapy System Epilepsy Physician's Manual*, Apr. 2021.

[122] R. El Tahry *et al.*, "Evolution in vns therapy for refractory epilepsy, experience with demipulse devices at ghent university hospital," *Seizure*, vol. 19, no. 9, pp. 531–535, 2010.

[123] LivaNova USA Inc., "Specifications: SenTiva generator M1000," http://www.neurosurgeryresident.net/Op.%20Operative%20Techniques/00.%20Catalogs,%20Brochures,%20Manuals/LivaNova/LivaNova%20-%20SenTiva.pdf, 2017.

[124] MicroTransponder, *Physician's Manual Paired VNS Therapy Serenity System Model 1000 Generator & Model 3000 Lead*, Sep. 2012.

[125] MicroTransponder Inc., "Pivotal study of vns during rehab after stroke (VNS-REHAB)," https://clinicaltrials.gov/ct2/show/NCT03131960, Mar. 2022.

[126] University of Glasgow, "Doctors aim to help stroke patients overcome disability by helping rewire their brains," https://www.gla.ac.uk/news/archiveofnews/2013/january/headline_259468_en.html, 2013, Accessed on: July 26, 2022.

[127] St. Jude Medical, "PMA P140009: FDA summary of safety and effectiveness data," https://www.accessdata.fda.gov/cdrh_docs/pdf14/P140009b.pdf, Jun. 2015.

[128] St. Jude Medical, "St. jude medical gets CE mark for deep brain stimulation device to treat dystonia," https://www.mddionline.com/, Apr. 2013.

[129] B. Scientific, *Vercise Deep Brain Stimulation Physician Manual 92093580-01*, 2017.

[130] B. Scientific, *Vercise Deep Brain Stimulation Physician Manual 91098825-07*, 2016.

[131] Boston Scientific, "Boston scientific announces ce mark for the vercise primary cell deep brain stimulation system," https://news.bostonscientific.com/, Sep. 2015.

[132] B. Scientific, "Vercisepc deep brain stimulation system," https://www.bostonscientific.com/content/dam/Boston%20Scientific%20Brazil/documentos/neurocirurgia/NM_305625_AB_Vercise_PC_Spec_Sheet_FINAL.pdf, 2015.

[133] Boston Scientific, "Boston scientific receives ce mark for vercise gevia deep brain stimulation system," https://news.bostonscientific.com/, Jun. 2017.

[134] Y. X., S. K., and M. R., "Characterizing rechargeable IPG charge cycle time in DBS," https://movementdisorders.ufhealth.org/x/movement/dbs-battery-estimator/activapc.html.

[135] B. Scientific, "Vercise genus deep brain stimulation system," https://www.bostonscientific.com/content/dam/bostonscientific/neuro/portfolio-group/Vercise%20Deep%20Brain%20Stimulation/MediaKit/documents/NM-765705%20INTL%20DBS%20Genus%20Spec%20Sheet_FINAL.pdf.

[136] Boston Scientific, "Boston scientific launches vercise genus DBS system in europe," https://www.bostonscientific.com/en-EU/news/newsroom-uk.html, Sep. 2020.

[137] Medtronic, "Summary of data from the medtronic post-market registry," http://www.medtronic.me/content/dam/medtronic-com/products/product-performance/ppr-reports/2020-dbs-product-performance-report.pdf?bypassIM=true, Mar. 2020.

[138] Medtronic, *System Eligibility - Battery Longevity - Deep brain stimulation systems*, 2021.

[139] UF Center for Movement Disorders & Neurorestoration, "Activasc battery life estimator," https://movementdisorders.ufhealth.org/x/movement/dbs-battery-estimator/activasc.html, Accessed on: July 26, 2022.

[140] St. Jude Medical, "Infinity - model names and differences," https://fccid.io/RIASJMRFC/Attestation-Statements/Model-Differences-Letter-3006422.pdf, May 2016.

[141] Abbott Medical Inc., "Infinity - summary of safety and effectiveness data (ssed)," https://www.accessdata.fda.gov/cdrh_docs/pdf14/P140009S039B.pdf, Jan. 2020.

[142] St. Jude Medical, "St. jude medical receives CE mark for the new infinity deep brain stimulation system and directional DBS lead," https://www.meddeviceonline.com/, Sep. 2015.

[143] St. Jude Medical, "Infinity dbs system," https://braininitiative.nih.gov/sites/default/files/pdfs/infinity_dbs_device_information_508c.pdf.

[144] Medtronic, "Activa PC - summary of safety and effectiveness data (SSED)," https://www.accessdata.fda.gov/cdrh_docs/pdf/P960009S219b.pdf, 2018.

[145] A. Sette *et al.*, "Battery longevity of neurostimulators in parkinson disease: a historic cohort study," *Brain stimulation*, vol. 12, no. 4, pp. 851–857, 2019.

[146] D. Haci, Y. Liu, S. S. Ghoreishizadeh, and T. G. Constandinou, "Key considerations for power management in active implantable medical devices," in *2020 IEEE 11th Latin American Symposium on Circuits & Systems (LASCAS)*. IEEE, 2020, pp. 1–4.

[147] U. C. for Movement Disorders & Neurorestoration, "Activa PC battery life estimator," https://movementdisorders.ufhealth.org/x/movement/dbs-battery-estimator/activapc.html, Accessed on: July 26, 2022.

[148] Medtronic, *Activa RC Multi-program rechargeable neurostimulator - Implant manual*, 2008.

[149] A. Goyal *et al.*, "The development of an implantable deep brain stimulation device with simultaneous chronic electrophysiological recording and stimulation in humans," *Biosensors and Bioelectronics*, vol. 176, p. 112888, 2021.

[150] Medtronic, "Percept PC neurostimulator with brainsense technology," https://www.medtronic.com/us-en/healthcare-professionals/products/neurological/deep-brain-stimulation-systems/percept-pc.html, Accessed on: July 26, 2022.

[151] Medtronic, "Percept PC clinician brochure," https://europe.medtronic.com/content/dam/medtronic-com/xd-en/hcp/documents/dbs/dbs-percept-hcp-brochure-final.pdf.

[152] Medtronic, "Medtronic receives CE mark approval for the Percept PC neurostimulator DBS system with brainsense technology," https://www.globenewswire.com/, Jan. 2020, Accessed on: March 10, 2022.

[153] NeuroPace, "Neuropace - summary of safety and effectiveness data (SSED)," https://www.accessdata.fda.gov/cdrh_docs/pdf10/p100026b.pdf, Feb. 2013.

[154] Medtronic, "Interstim product catalogue," https://europe.medtronic.com/content/dam/medtronic-com/xd-en/hcp/documents/pelvic-health/interstim-product-catalogue.pdf, 2020.

[155] Medtronic, "Medtronic receives FDA approval for InterStimX system, the next generation of the most personalized sacral nerve stimulation therapy for bladder and bowel control," https://news.medtronic.com/, Feb. 2022, Accessed on: July 26, 2022.

[156] B. F. Blok, "Sacral neuromodulation for the treatment of urinary bladder dysfunction: mechanism of action and future directions," *Bioelectronics in Medicine*, vol. 1, no. 1, pp. 85–94, 2018.

[157] Axonics, *Sacral Neuromodulation System Neurostimulator - Implant manual*, 2019.

[158] R. L. Poole, M. Dale, H. Morgan, T. Oladapo *et al.*, "Axonics sacral neuromodulation system for treating refractory overactive bladder: a nice medical technologies guidance," *Applied Health Economics and Health Policy*, pp. 1–9, 2021.

[159] D. S. Elterman, "The novel axonics® rechargeable sacral neuromodulation system: procedural and technical impressions from an initial north american experience," *Neurourology and urodynamics*, vol. 37, no. S2, pp. S1–S8, 2018.

[160] Medtronic, *Intellis Rechargeable neurostimulator - Implant manual*, Jun. 2016.

[161] Medtronic, "Intellis with adaptivestim technology Intellis rechargeable neurostimulators," https://www.medtronic.com/us-en/healthcare-professionals/products/neurological/spinal-cord-stimulation-systems/intellis-platform.html, Accessed on: July 26, 2022.

[162] Medtronic, "Medtronic wins CE mark for Intellis SCS, PNS systems," https://www.massdevice.com/, Nov. 2017, Accessed on: July 26, 2022.

[163] Medtronic, "Summary of data from the medtronic post-market registry," http://www.medtronic.me/content/dam/medtronic-com/products/product-performance/ppr-reports/2019-spinal-cord-stimulation-report.pdf, Mar. 2020.

[164] St. Jude Medical, "Eon mini rechargeable IPG," https://www.cardion.cz/file/447/eonmini-specifikace.pdf, 2008.

[165] MED DEVICE ONLINE, "St. Jude Medical receives FDA and CE mark approvals for rechargeable neurostimulator to treat chronic pain," https://www.meddeviceonline.com/, Apr. 2008, Accessed on: July 26, 2022.

[166] Medtronic, *RestoreUltra SureScan MRI Rechargeable neurostimulator - Implant manual*, 2013.

[167] Medtronic, *RestoreSensor Multi-program rechargeable neurostimulator - Implant manual*, Mar. 2011.

[168] Medtronic, *PRIMEADVANCED Multi-program neurostimulator - Implant Manual*, 2006.

[169] Medtronic, *RestoreAdvanced® SureScan® MRI Rechargeable neurostimulator - Implant manual*, 2013.

[170] Medtronic, *Itrel 4 Programmable neurostimulator - Implant Manual*, 2012.

[171] Advanced Bionics Corporation, *Precision Spinal Cord Stimulation System - Physician Implant Manual*, 2003.

[172] Boston Scientific, *Precision Montage MRI 16 Contacts Implantable Pulse Generator - Directions for Use*, 2016.

[173] Boston Scientific, *Precision Novi Implantable Pulse Generator - Directions for Use*, 2017.

[174] Boston Scientific, *Precision Plus Rechargeable Spinal Cord Stimulation System*, 2013.

[175] St. Jude Medical, *Implantable Pulse Generator Prodigy IPG - Clinician's Manual*, 2016.

[176] St. Jude Medical, "Prodigy MRI SCS device information," https://braininitiative.nih.gov/sites/default/files/pdfs/prodigy_mri_scs_device_information_508c.pdf.

[177] St. Jude Medical, *Proclaim Implantable Pulse Generator Clinician's Manual*, Feb. 2017.

[178] Abbott Laboratories, "Proclaim XR recharge-free SCS system," https://www.neuromodulation.abbott/us/en/hcp/products/spinal-column-stimulation-for-chronic-pain/proclaim-xr-scs-system/ht-tab/tech-specs.html, Accessed on: July 26, 2022.

[179] NEVRO, *Physician Implant Manual*, 2015.

[180] NEVRO, "PMA P130022: FDA summary of safety and effectiveness data," https://www.accessdata.fda.gov/cdrh_docs/pdf13/P130022b.pdf, 2015.

[181] NEVRO, "Form 10K: Annual report pursuant to section 13 or 15(d) of the securities exchange act of 1934," https://materials.proxyvote.com/default.aspx?docHostID=354064, 2017, Accessed on: July 26, 2022.

[182] +MassDevice, "Saluda Medical wins CE mark for Evoke closed-loop SCS," https://www.massdevice.com/, Sep. 2019, Accessed on: July 26, 2022.

[183] Inspire, *Inspire - System Implant Manual*, 2014.

[184] Respicardia Inc., "PMA P160039: Summary of safety and effectiveness data (SSED)," https://www.accessdata.fda.gov/cdrh_docs/pdf16/P160039b.pdf, Oct. 2017.

[185] Respicardia Inc., *The remede System Implant and Clinician Use Manual*, 2010.

[186] Medtronic, *ADVISA DR MRI SURESCAN A3DR01, ADVISA SR MRI SURESCAN A3SR01 - Clinician Manual*, 2014.

[187] Medtronic, *Azure XT SR MRI SureScan W2SR01 - Device Manual*, 2017.

[188] Medical Device Network, "Medtronic introduces new pacemakers in us," https://www.medicaldevice-network.com/news/, Nov. 2017, Accessed on: July 26, 2022.

[189] Medtronic, "FDA approves next generation medtronic leadless pacemaker," https://www.medtronic.com/us-en/index.html, Jan. 2020, Accessed on: July 26, 2022.

[190] B. Scientific, *Pacemaker - Physician's technical manual*, 2018.

[191] Boston Scientific, "Press release first implant of boston scientific vitalio pacemaker takes place in europe," https://www.bostonscientific.com/en-EU/news/newsroom-uk.html, Jan. 2013.

[192] MicroPort, *ENO DR / ENO SR - IMPLANT MANUAL*, 2018.

[193] MicroPort, *TEO DR / TEO SR - IMPLANT MANUAL*, 2018.

[194] MicroPort, *OTO DR / OTO SR - IMPLANT MANUAL*, 2018.

Santiago Martínez (S'22) received the Electrical Engineering degree from Universidad de la República, Uruguay in 2011 and the MSc. degree from the same university in 2018. His thesis concerned the development of a programmable logic based control unit for implantable neurostimulation circuits. He is a PhD student from Universidad de la República, Uruguay and his research area concerns energy efficiency in implantable devices, particularly in ultra low power digital circuits. He is currently Assistant Professor at the Electrical Engineering Department of the School of Engineering of Universidad de la República, Uruguay, activity in which he is involved part-time since 2011. He is senior Engineer at the R&D department of CCC Medical Devices, part of Integer Holdings Corporation (CRM and Neuromodulation), since 2012. In the last decade, he has been involved in design, risk analysis and design verification activities for 15 implantable class III devices.
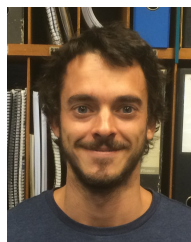
Francisco Veirano (M'12) received the Electrical Engineering degree from Universidad de la República, Uruguay in 2013 and PhD degree 2019 from the same university. He joined the Electrical Engineering Department of Universidad de la República, Uruguay in 2012 where he is currently working as Assistant Professor. His research interests include ultra low-power analog and digital integrated circuits design, specially focus on sub threshold digital circuits and the power management associate with these circuits.

Timothy G. Constandinou (AM'98–M'01–SM'10) received the B.Eng. and Ph.D. degrees in electronic engineering from Imperial College London, in 2001 and 2005, respectively. He is currently Professor of Bioelectronics at Imperial College London, Director of the Next Generation Neural Interfaces (NGNI) Lab and Head of the Circuits & Systems (CAS) Research Group. He is also a Group Leader within the UK Dementia Research Institute, Care Research & Technology Centre. His research interests are in biomedical microsystems, implantable medical devices, neural interfaces, brain-machine interfaces, research platforms, and remote sensing using ultra-wideband radar. His lab focuses on creating innovative neurotechnologies to enable communication between the nervous system and electronic devices to study, manage, or treat neurological conditions. He recently co-founded MintNeuro, an Imperial College spinout to translate his research in the field of implantable neurotechnology. Within the IEEE, he regularly serves on Circuits and Systems (CAS) Society conference committees including Technical Program Co-Chair (BioCAS 2010, 2011, 2018), General Chair (BrainCAS 2016, NeuroCAS 2018), Plenary Co-Chair (ICECS 2020, ICECS 2022), Special Session Co-Chair (ISCAS 2017, BioCAS 2019), Tutorial Co-Chair (ISCAS 2021, BioCAS 2022, BioCAS 2024). Previously he served on the IEEE Circuits and Systems (CAS) Society, Board of Governors (2017–19) and was Associate Editor-in-Chief of IEEE Transactions on Biomedical Circuits and Systems (2020-21).

Fernando Silveira (S'89–M'90–SM'03) received the degree in electrical engineering from the Universidad de la República, Montevideo, Uruguay, in 1990, and the M.Sc. and Ph.D. degrees in microelectronics from the Universitè catholique de Louvain, Louvain-la-Neuve, Belgium, in 1995 and 2002, respectively. He is currently a Professor with the Electrical Engineering Department, Universidad de la República. His current research interests include the design of ultra low-power analog and RF integrated circuits and systems, in particular with biomedical application. In this field, he has co-authored two books and many technical papers. He has had multiple industrial activities including leading the design of an application specific integrated circuit for implantable pacemakers and designing analog circuit modules for implantable devices for various companies worldwide. He served as IEEE CASS Distinguished Lecturer (2011 - 2012), Associate Editor of IEEE TCAS II (2020 - 2021) and member of Senior Editorial Board of JETCAS (2022 - 2023).